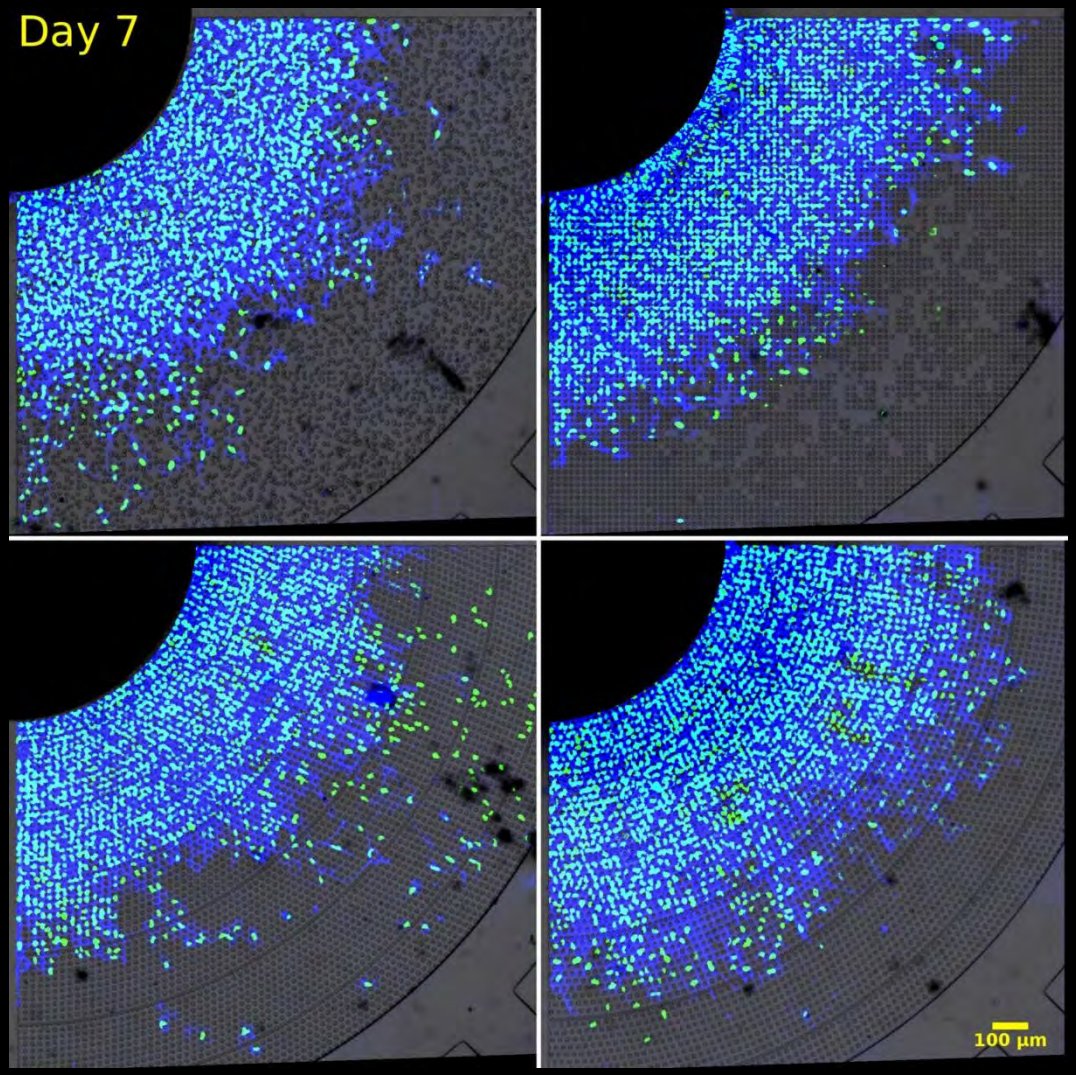

Theoretical models of collective cell motion

Edouard Hannezo

Collective motion at the mesoscale in biology

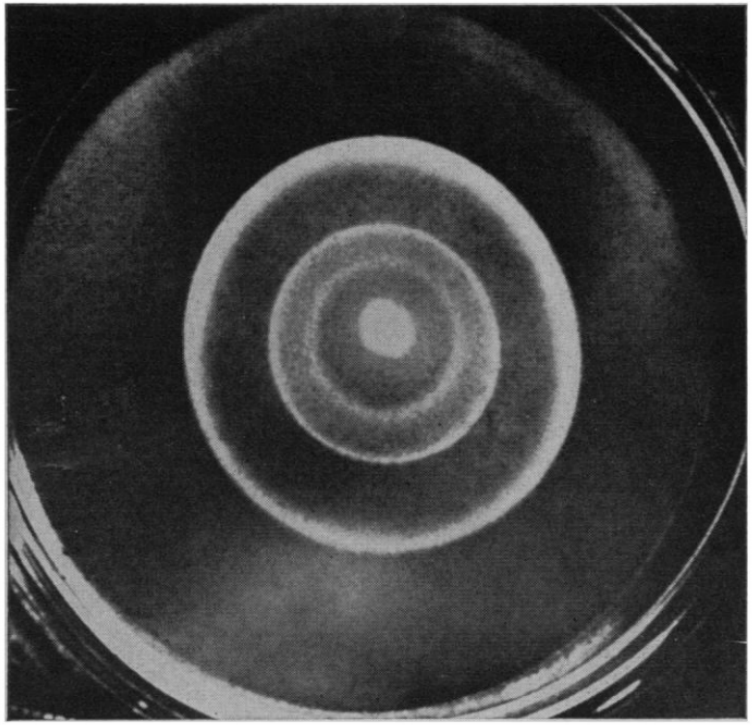

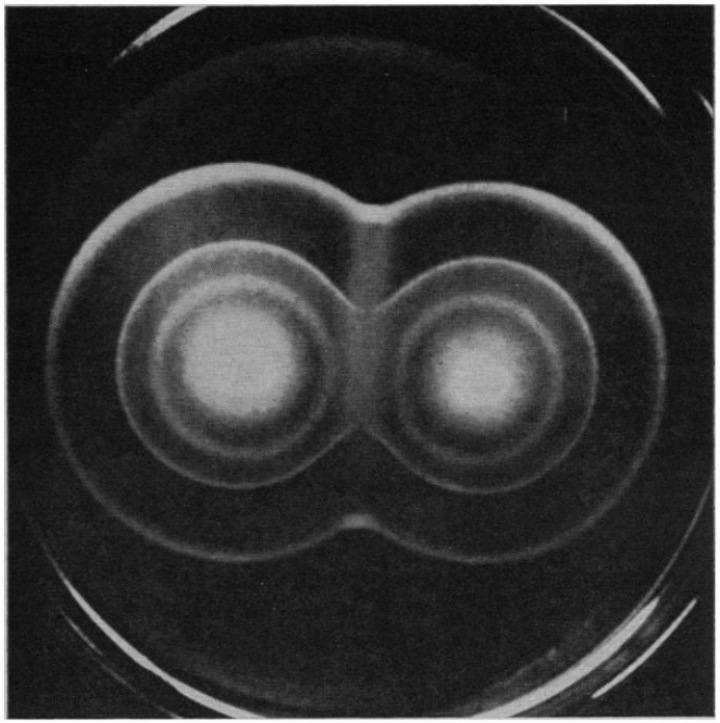

Figs. 14 and 15. Fig. 14 (left). Three rings of *Escherichia coli* in a tryptone-agar plate after 5 hours of incubation at 37°C. About 10^8 motile cells were deposited at the center of a plate containing Difco tryptone (10 g/liter), sodium chloride (5 g/liter) and agar (2 g/liter). [Photograph by John L. Tschernitz] Fig. 15 (right). A suspension of motile *Escherichia coli* deposited at two places on the surface of a tryptone-agar plate swarms out in rings that stop when they meet. [Photograph by John L. Tschernitz]

Adler, Science, 1966

E. Coli migrates/expands in bands when locally platted on a dish

Collective motion at the mesoscale in biology

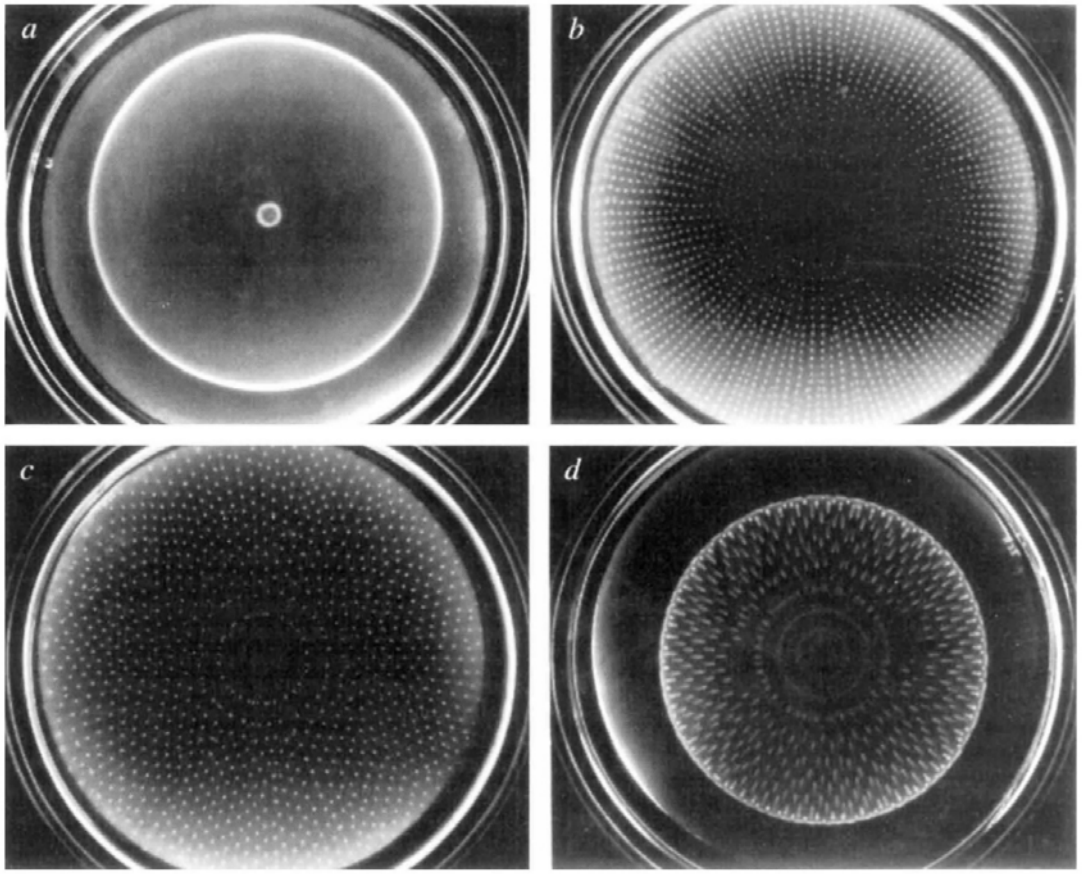

Budrene and Berg, Nature, 1995

Rich patterns of colony growth can be seen when changing the experimental conditions/bacterial strain

Collective motion at the mesoscale in biology

Čejková J. (2013)

Slime mold/social amoebae aggregation (Dictyostelium)

Finding the right direction: how is directed cell migration encoded?

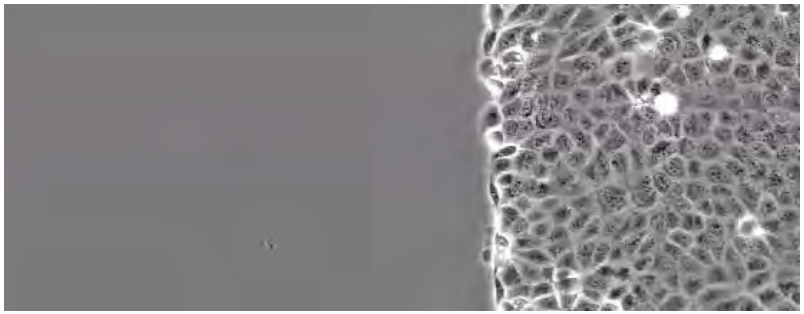

MDCK, phase contrast, Hino et al, Dev Cell, 2020
See also works from the Silberzan, Ladoux, Trepat groups.

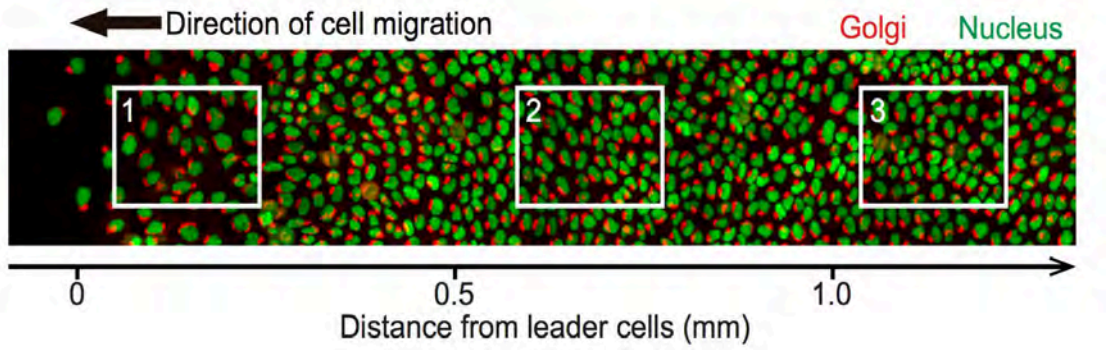

Where does long-range polar order come from?

Finding the right direction: how is directed cell migration encoded?

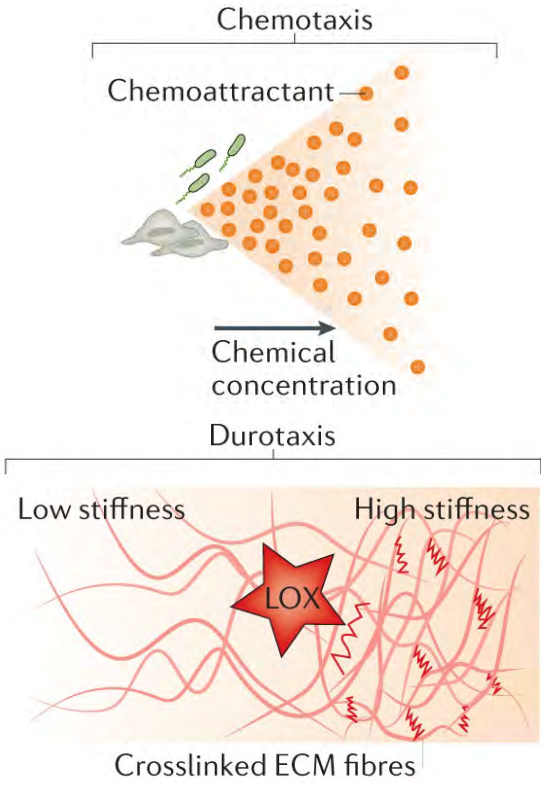

Sengupta et al, Nat Rev Mol Cell Biol, 2021

Classical view: cells can move up gradients of signals (diffusible molecules, but also stiffness/electric fields/friction etc)…

But where does the gradient come from in most situations?

Directional migration via self-generated gradients

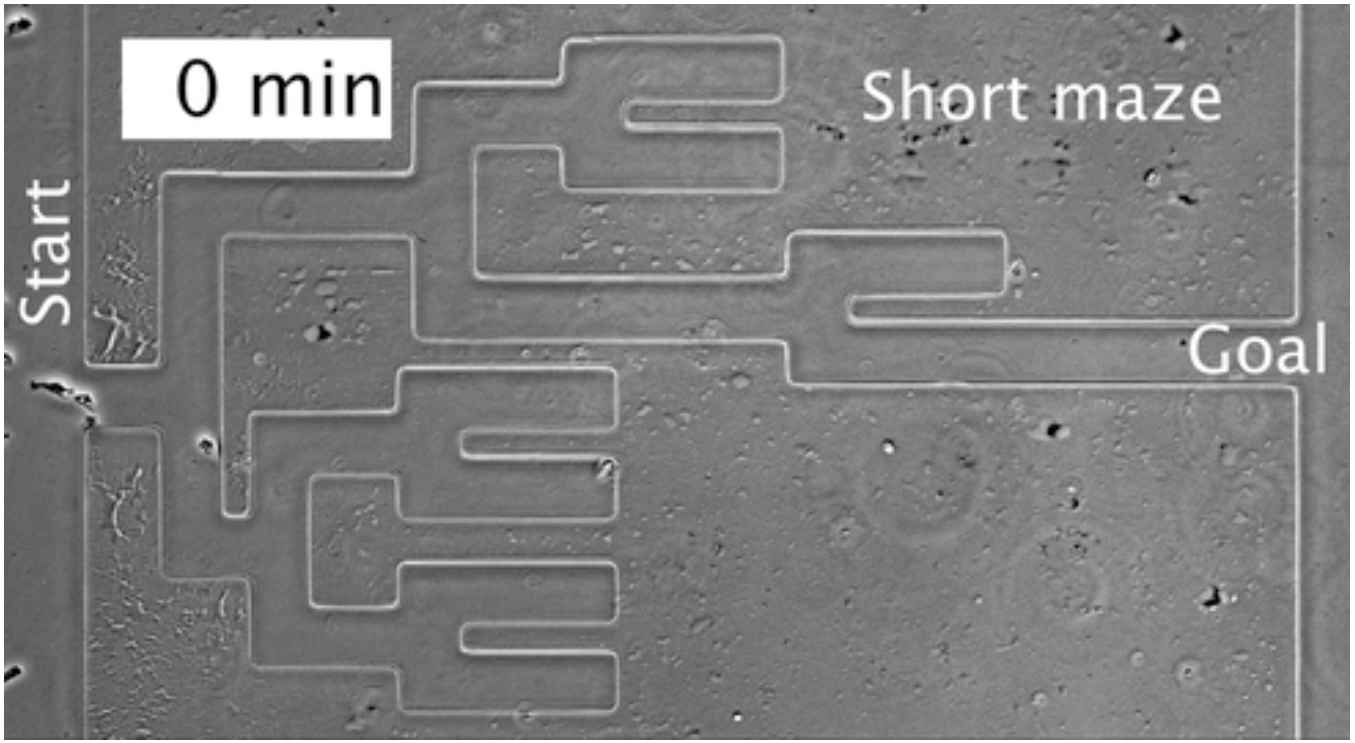

Twieedy and Insall, 2020

Cells can collectively solve mazes via cell migration in the absence of pre-patterned gradients!

Emergence of global polar order in biology

3D « flocks » of birds

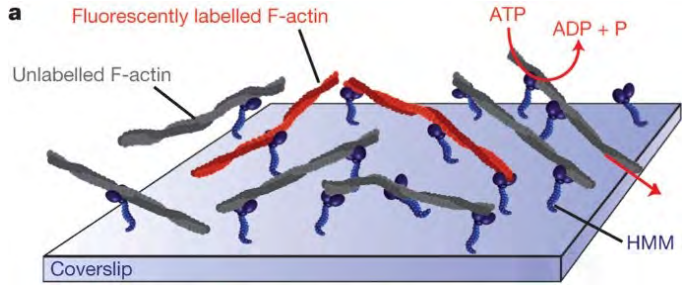

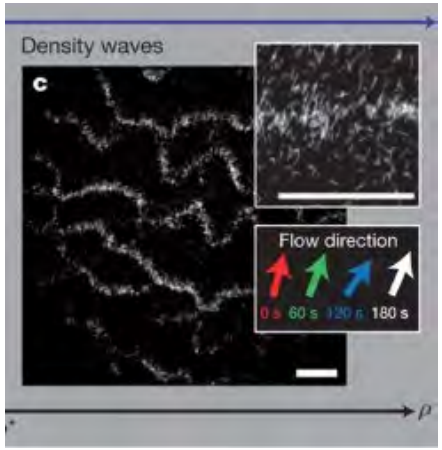

Schaller et al, Nature, 2010

Global ordering of active self-propelled objects

Collective cell migration and active matter models

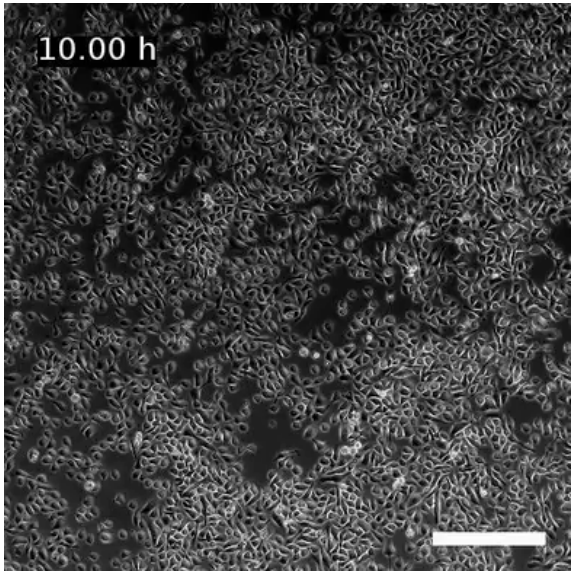

Garcia et al, PNAS, 2015

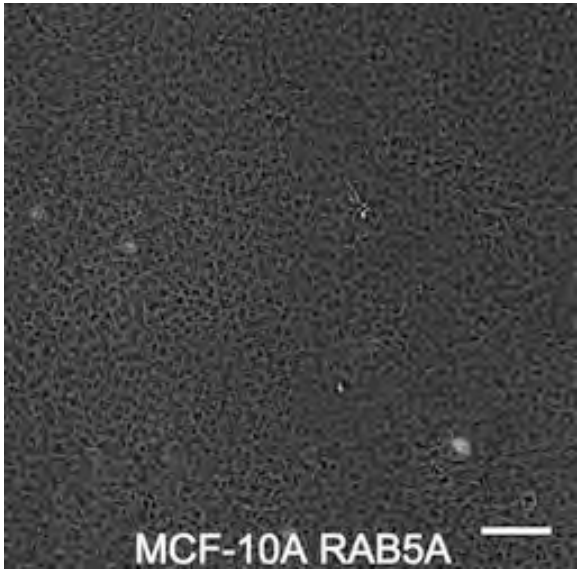

Malinverno et al, Nat Mat, 2017

Complex spatio-temporal patterns observed in minimal *in vitro* systems of **homogeneous cells migrating on flat 2D substrates**…

Extensive comparisons to active matter theories in the past decade (e.g. flocking, active glasses, nematic turbulence etc)

E.g. Banerjee et al,, 2015, Blanc-Mercader et al, 2017, Notbohm et al, 2017, Tlili et al, 2018, Petroli et al, 2019, Henkes et al, 2020, Alert & Trepat, 2020

Part 1: Directional migration via self-generated chemokine gradients

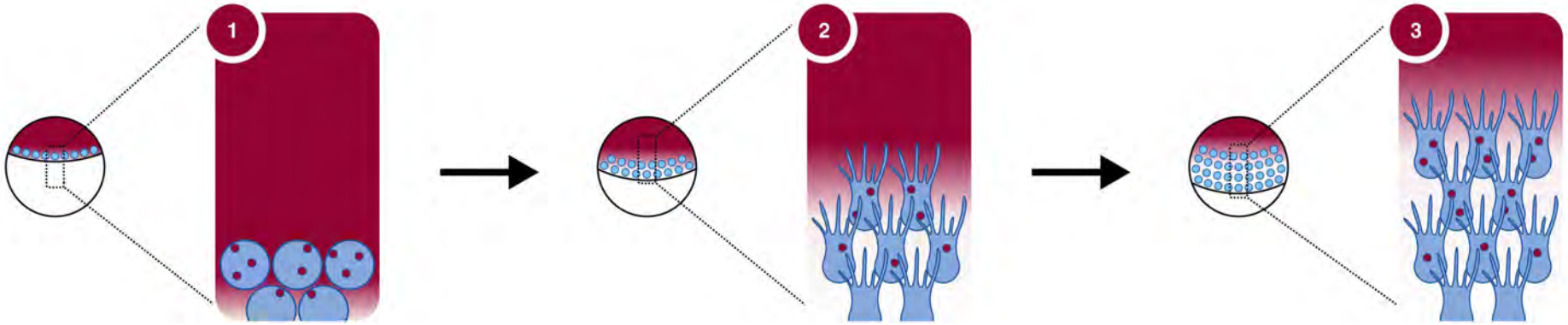

Stock et al, Sci Adv, 2022

Cells can self-generate gradients by consuming their own chemoattractant

Dona et al, Cell, 2013, Tweedy et al, Science 2020, Stock et al, Sci Adv, 2021, Alanko et al, Sci Immuno, 2022

Can different cell types communicate directionality to each other via a diffusible signal?

See also Agudo-Canalejo and Golestanian, PRL, 2019

Part 1: Directional migration via self-generated chemokine gradients

Michael Sixt

Zane Alsberga

Mehmet Ucar
→ Sheffield

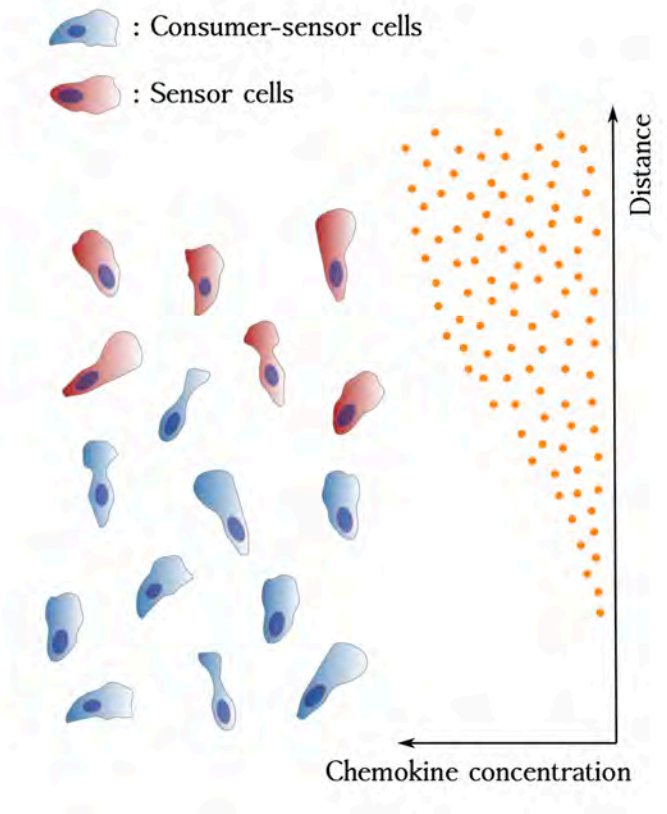

Dendritic cells (DC) self-generated their own gradients (Alanko et al, 2022), but most other immune cell types might not…

Could they « surf » on the gradients from DC cells? Are there optimal principles for co-migration of multiple cell populations?

Optimal principles for co-migration of multiple cell populations

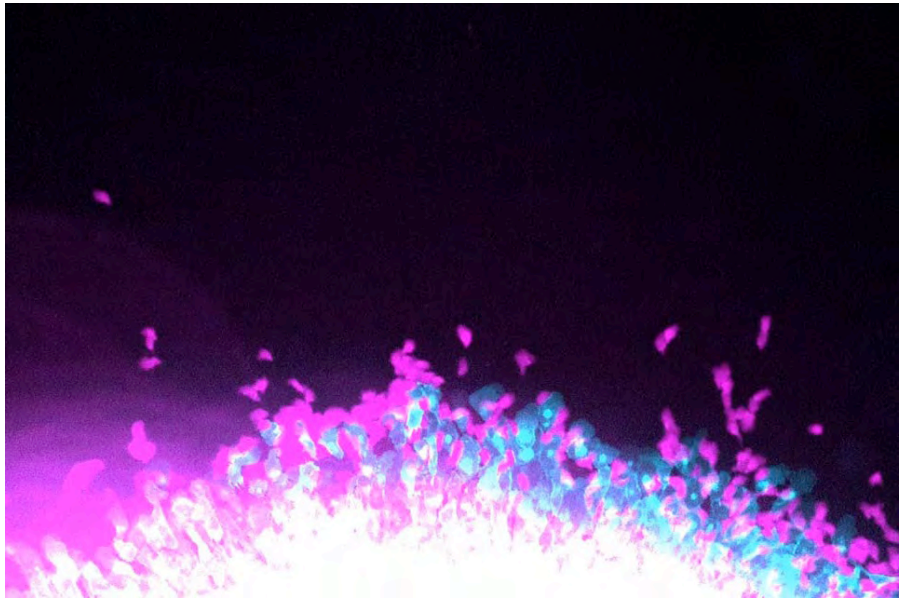

T cells, Dendritic cells

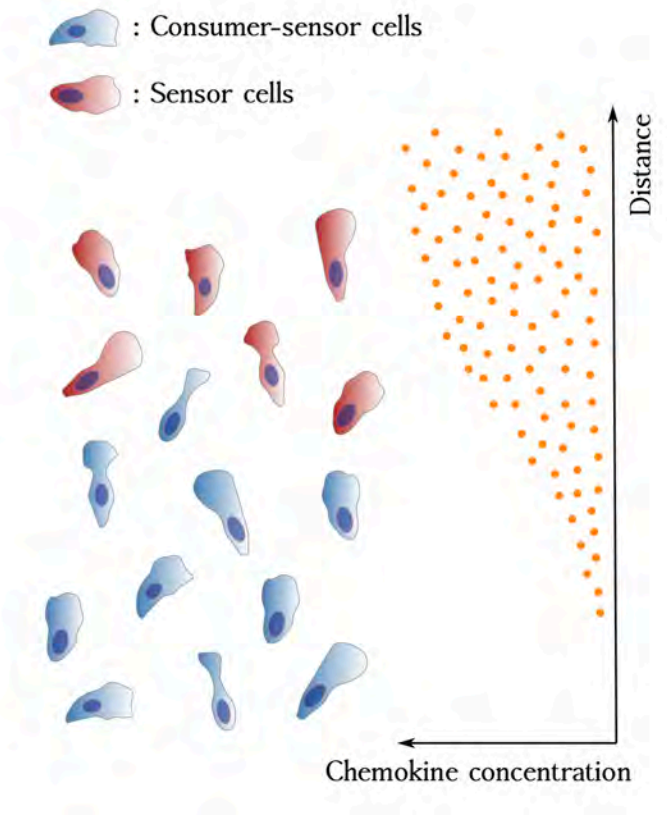

In vitro experiments in presence of an initially uniform chemoattractant show robust co-migration, with « sensors » in front.

Optimal principles for co-migration of multiple cell populations

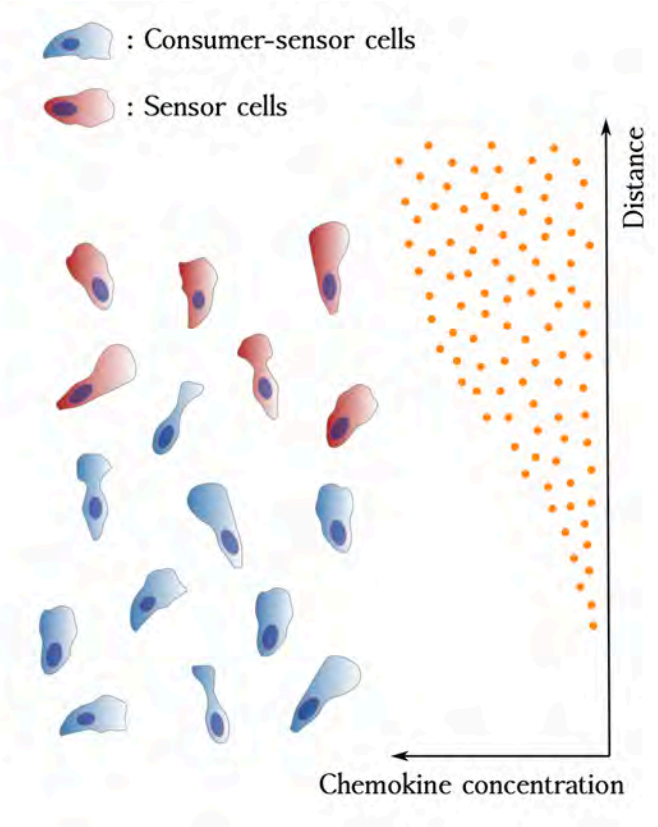

$$\partial_t \rho_i = \tilde{D}_i \nabla^2 \rho_i - \tilde{\chi}_i \nabla \cdot \left(\rho_i \frac{\nabla a}{a} \right)$$

$$\partial_t a = \nabla^2 a - \rho_c a$$

Theory of multiple cellular species i with diffusion D_i and chemotactic strength χ_i

One species c consumes the chemoattractant a

Optimal principles for co-migration of multiple cell populations

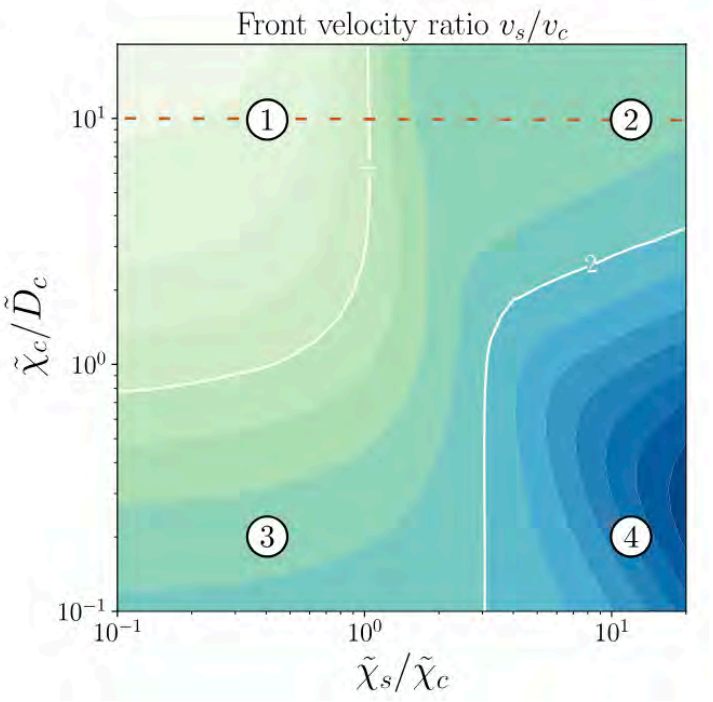

$$\partial_t \rho_i = \tilde{D}_i \nabla^2 \rho_i - \tilde{\chi}_i \nabla \cdot \left(\rho_i \frac{\nabla a}{a} \right)$$

$$\partial_t a = \nabla^2 a - \rho_c a$$

Theory of multiple cellular species i with diffusion D_i and chemotactic strength χ_i

One species c consumes the chemoattractant a

Essentially controlled by two rescaled parameters:

- χ_c/D_c (advection/diffusion of the consumer)
- χ_s/χ_c (relative advection of sensor vs consumer)

Optimal principles for co-migration of multiple cell populations

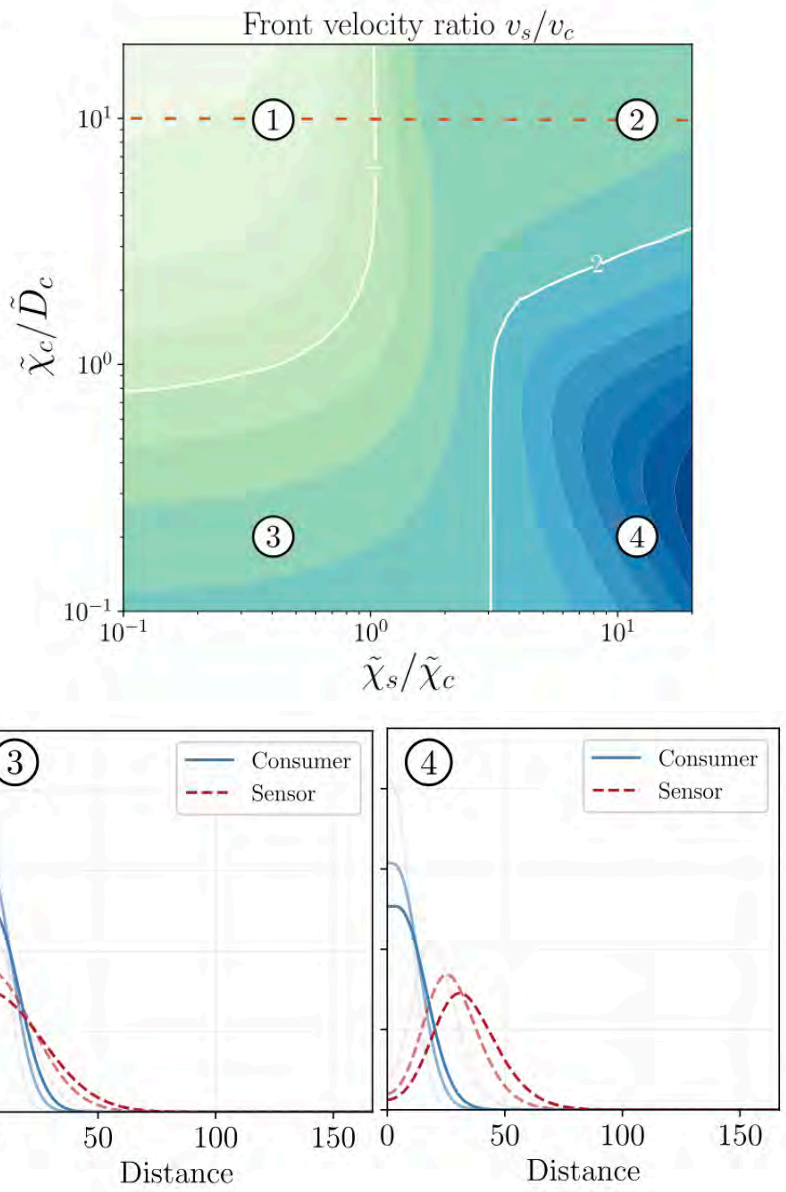

χ_c/D_c controls the peakedness of the distribution and the capacity for long-term travelling waves.

Optimal principles for co-migration of multiple cell populations

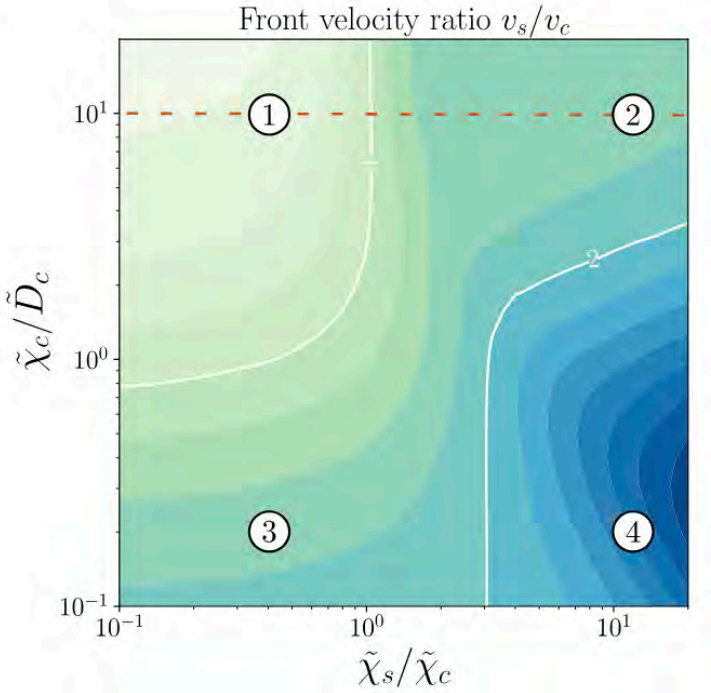

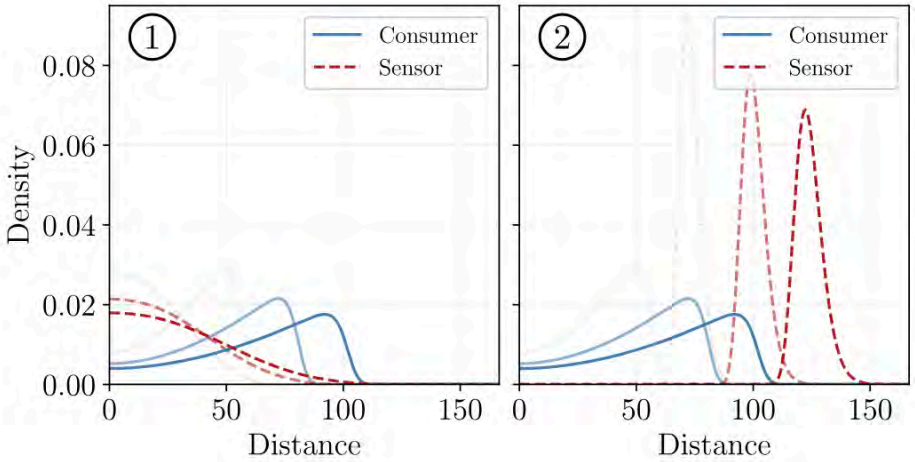

χ_c/D_c controls the peakedness of the distribution and the capacity for long-term travelling waves.

Sharp boundary for $\chi_s/\chi_c < 1$ (sensor population cannot keep up and falls behind).

Optimal principles for co-migration of multiple cell populations

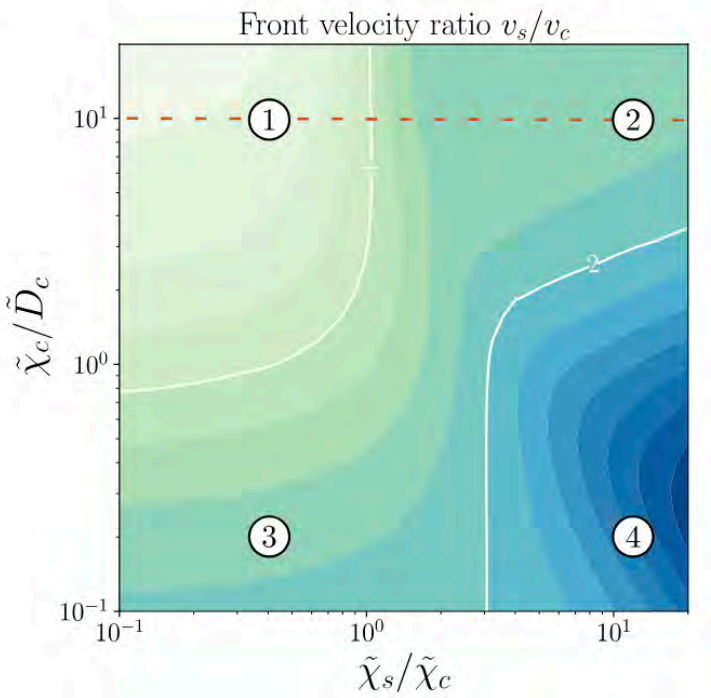

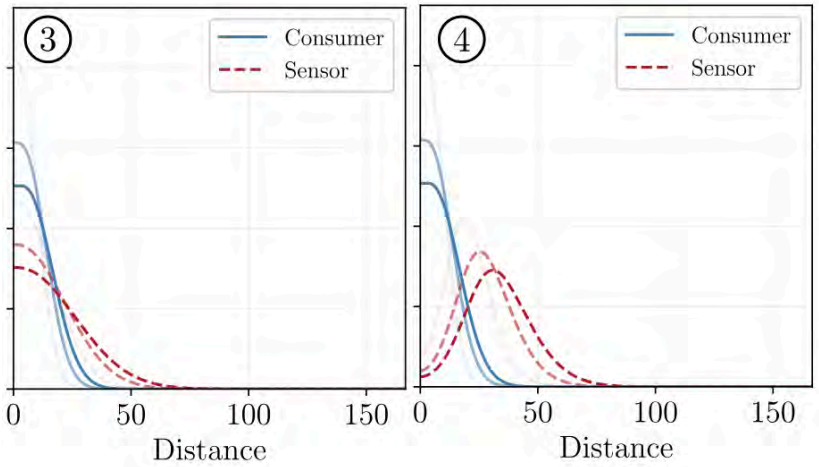

χ_c/D_c controls the peakedness of the distribution and the capacity for long-term travelling waves.

Sharp boundary for $\chi_s/\chi_c < 1$ (sensor population cannot keep up and falls behind).

For $\chi_s/\chi_c \gg 1$, speed of sensors still bounded by speed of consumers, but peaks farther and farther ahead.

Optimal principles for co-migration of multiple cell populations

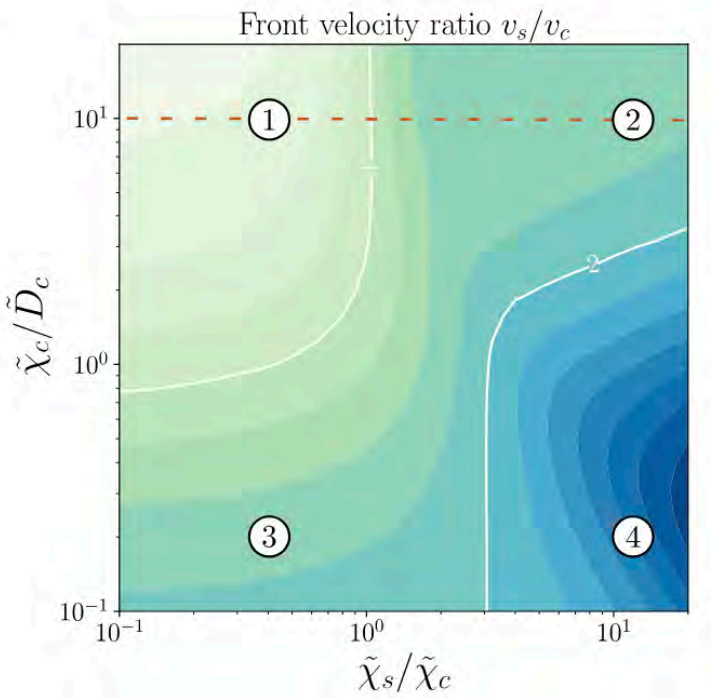

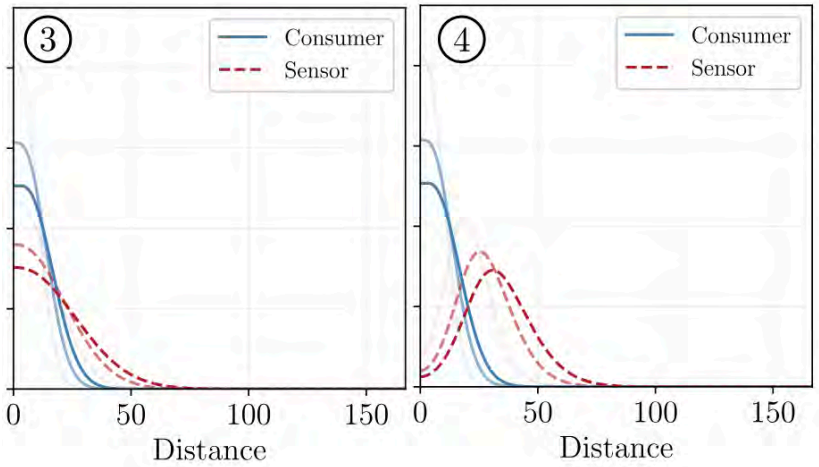

χ_c/D_c controls the peakedness of the distribution and the capacity for long-term travelling waves.

Sharp boundary for $\chi_s/\chi_c < 1$ (sensor population cannot keep up and falls behind).
For $\chi_s/\chi_c \gg 1$, speed of sensors still bounded by speed of consumers, but peaks farther and farther ahead.

Analytics for speed of propagation:

$$\mathcal{V} = \chi_c \sqrt{\frac{m\rho_c^\dagger}{D_a + \chi_c}}$$

Front of the pulse: $\rho_i \propto \exp(-\mathcal{V} z/\tilde{D}_i)$

Meaning that $\zeta_c/\zeta_s = D_s/D_c$

Quantitative comparison to experimental data

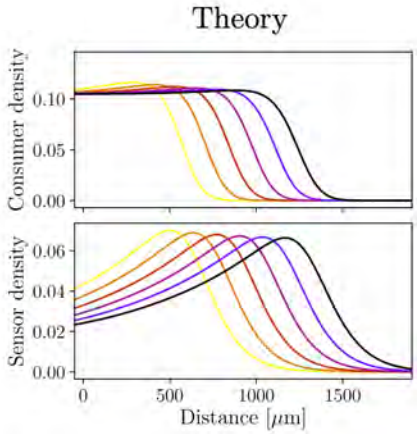

Most parameters can be extracted from independent experiments (e.g. single cell types, FRAP assay for chemoattractant).

$\chi_s/\chi_c \approx 1.5 - 3$
$\chi_c/D_c \approx 4 - 5$
$D_s/D_c \approx 3$

Quantitative comparison to experimental data

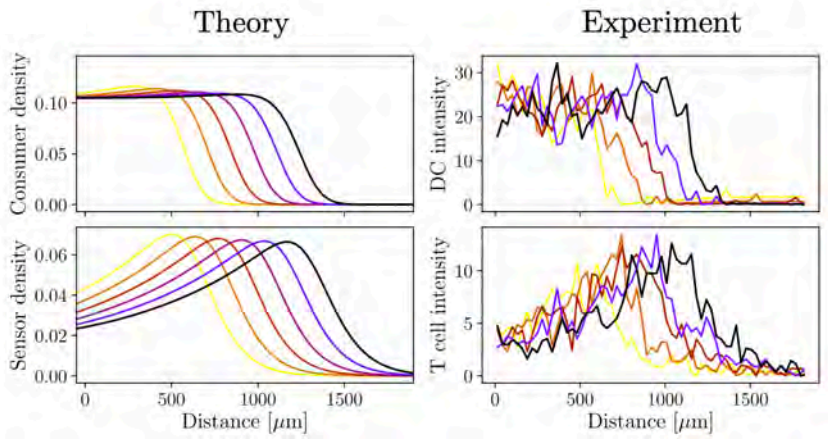

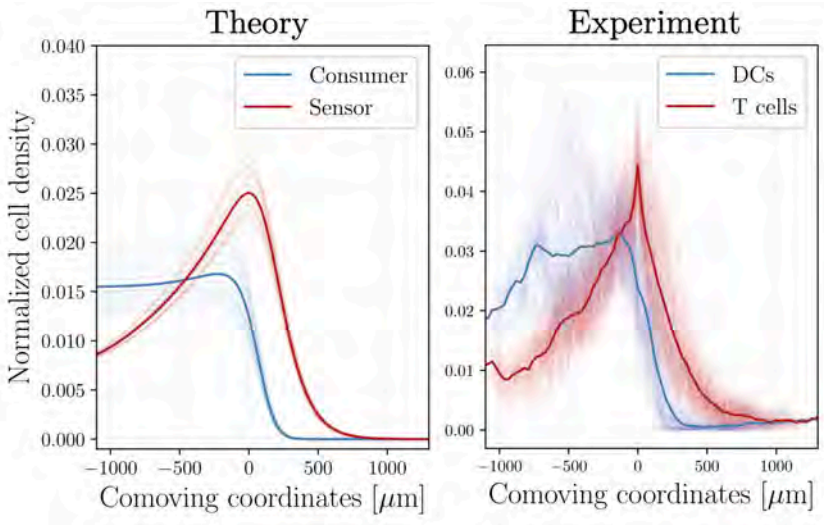

Most parameters can be extracted from independent experiments (e.g. single cell types, FRAP assay for chemoattractant).

$\chi_s/\chi_c \approx 1.5 - 3$
$\chi_c/D_c \approx 4 - 5$
$D_s/D_c \approx 3$

Good qualitative and quantitative agreement with data!

→ Peaked travelling waves with near constant spacing between the two populations

→ Analytical predictions for the back & front of the waves consistent with data

Conclusion 1: Tradeoffs between robust co-migration and co-localization during immune response

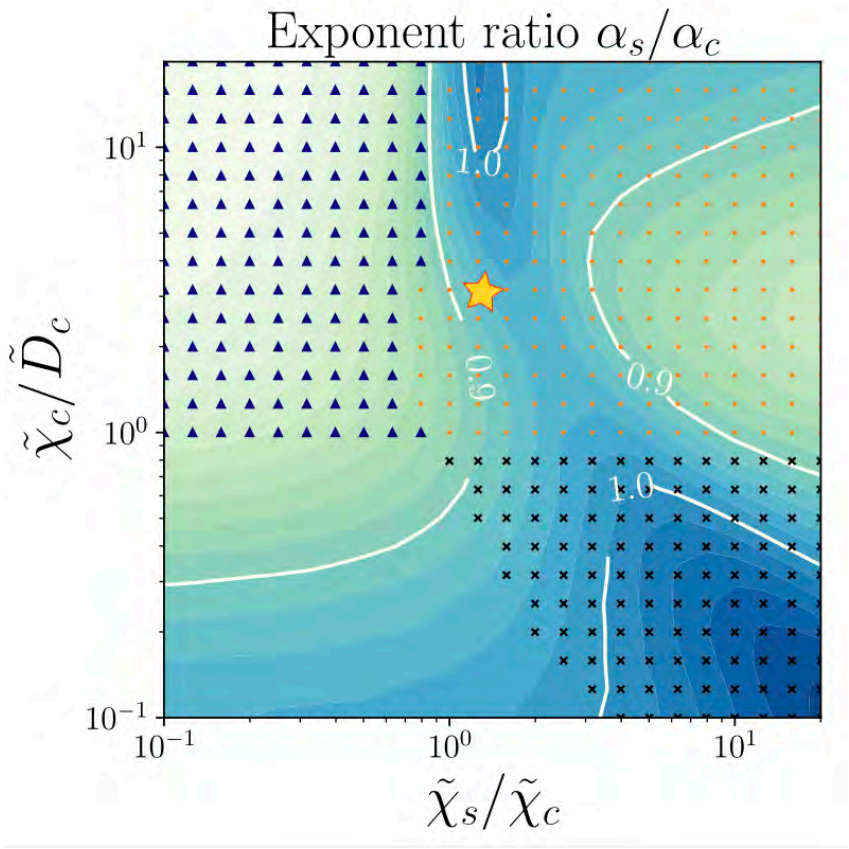

Trade-offs if immune cells want to interact/co-colocalize during migration (e.g. antigen presentation)

Intermediate region of parameter space that optimizes for both robust and colocalized co-migration?

Emergence of global polar order in biology

3D « flocks » of birds

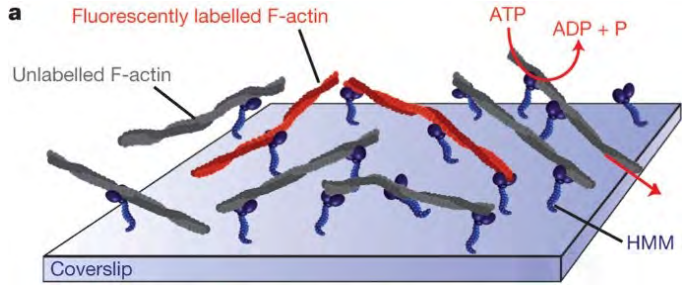

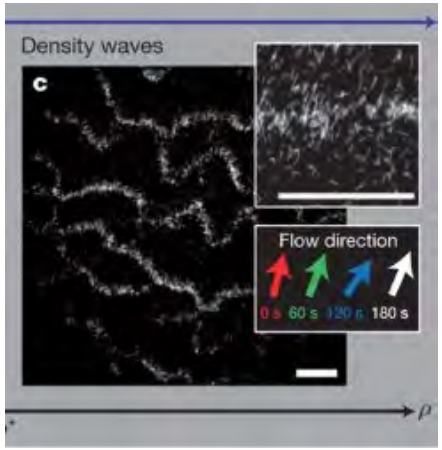

Schaller et al, Nature, 2010

Global ordering of active self-propelled objects

Vicsek model (1995) as a paradigm of active systems

3D « flocks » of birds

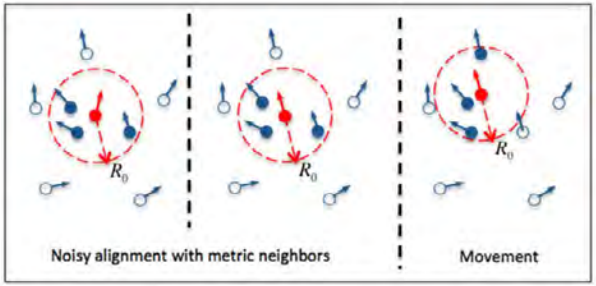

$$\begin{cases} \boldsymbol{r_i(t+dt) = r_i(t) + v_i(t)dt} \\ \boldsymbol{\theta_i(t+dt) =< \theta_j(t) > + \eta(t)} \end{cases}$$

where *j* is a neighbor list of *i* : $\boldsymbol{|r_i - r_j| < R_0}$

Animals as point particles with a spin.

White noise $\boldsymbol{\eta(t)}$ + Ising-like aligment term + movement $\boldsymbol{v_0}$ in the direction of the spin.

In 2D, let's define spin angle of particle *i* as $\theta_i(t)$, so that $v_i(t) = v_0(cos(\theta_i(t)), sin(\theta_i(t)))$

→ for $v_0 = 0$, this is simply the classical XY model!

Vicsek model (1995) as a paradigm of active systems

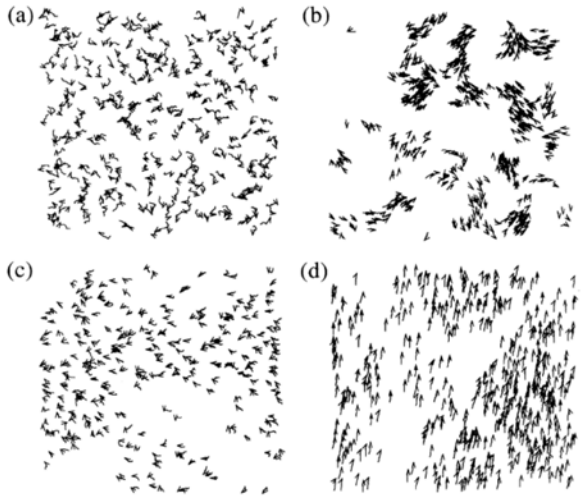

Vicsek, PRL, 1995

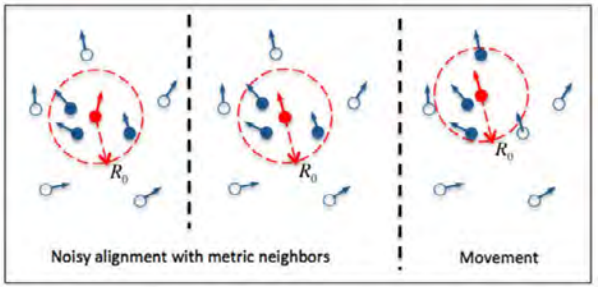

$$\begin{cases} \boldsymbol{r_i(t+dt) = r_i(t) + v_i(t)dt} \\ \boldsymbol{\theta_i(t+dt) = <\theta_j(t)> + \eta(t)} \end{cases}$$

where *j* is a neighbor list of *i* : $\boldsymbol{|r_i - r_j| < R_0}$

Model predicts emergence of **long-range orientational order** when interactions are large enough compared to noise

Vicsek model (1995) as a paradigm of active systems

Viscek model: continuum symmetry (as XY), finite noise, 2d… but still broken symmetry.

Clearly active **movements v_0** have to explain this (in fact singular transition for any $v_0 > 0$) … but how exactly?

First order transition, which occurs when density is large enough/noise low enough

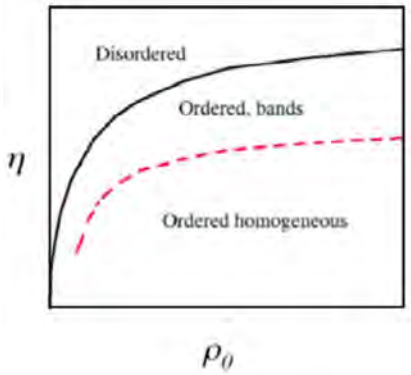

Vicsek model (1995) as a paradigm of active systems

First order transition, which occurs when density is large enough/noise low enough

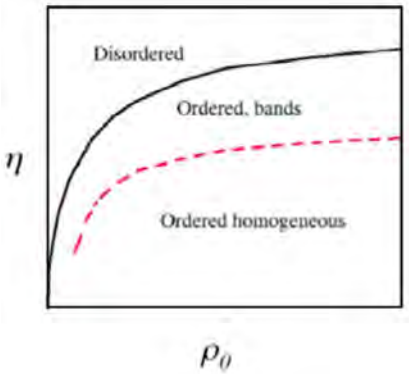

Simple mean field argument - at density ρ_0, velocity v_0 and noise η:

- Mean free path of a particle (between collisions) scales as $1/\rho_0$
- Particle looses spin orientation memory on length scales $\frac{v_0}{\eta^2}$

→Ordering can only happen if $\eta < \sqrt{v_0 \rho_0}$ (collisions more frequent than random re-orientation)

Good approximation for low densities

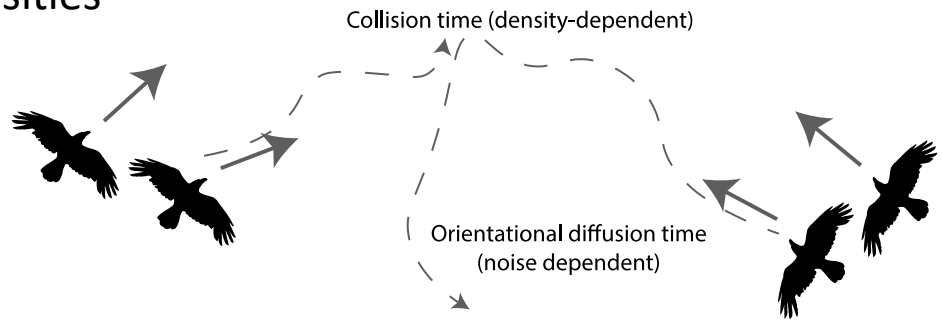

Ginelli et al, 2016

Collective cell migration and active matter models

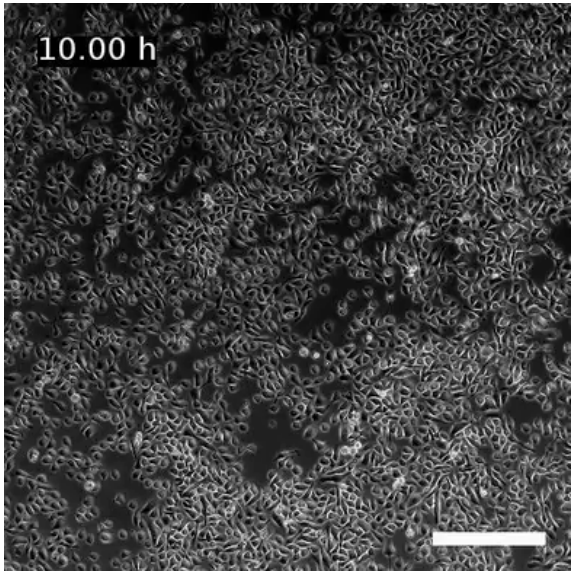

Garcia et al, PNAS, 2015

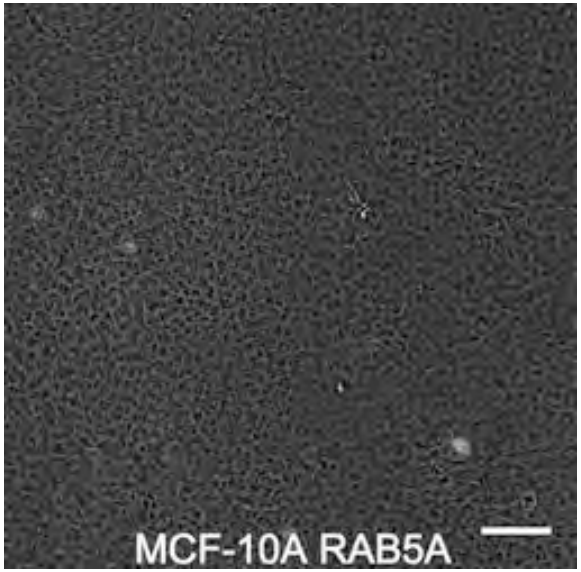

Malinverno et al, Nat Mat, 2017

Complex spatio-temporal patterns observed in minimal *in vitro* systems of **homogeneous cells migrating on flat 2D substrates**…

Extensive comparisons to active matter theories in the past decade (e.g. flocking, active glasses, nematic turbulence etc)

E.g. Banerjee et al,, 2015, Blanc-Mercader et al, 2017, Notbohm et al, 2017, Tlili et al, 2018, Petroli et al, 2019, Henkes et al, 2020, Alert & Trepat, 2020

Part 2: Geometry-driven migration efficiency of minimal cell clusters

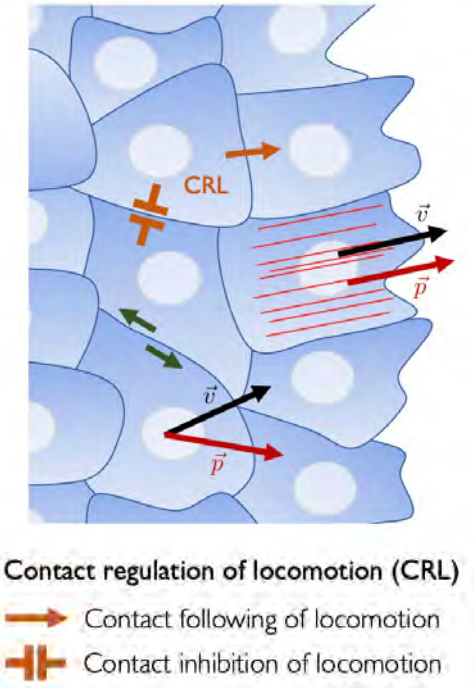

Alert & Trepat, 2020

Experimentally, different collective modes of motility **alignement or anti-alignement** in different cell types…

See also Veluda et al, 2012, Sepulveda et al, 2013, Basan et al, 2013, Camley et al, 2014, Bertrand et al, 2020, Bruckner et al, 2021, Ron et al, 2023

Geometry-driven migration efficiency of minimal cell clusters

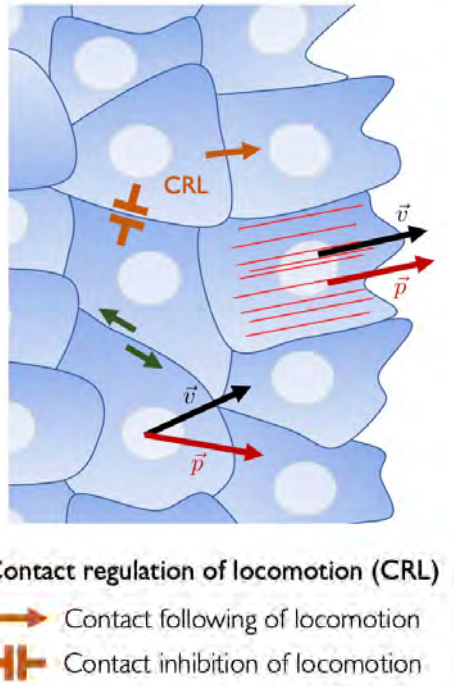

Alert & Trepat, 2020

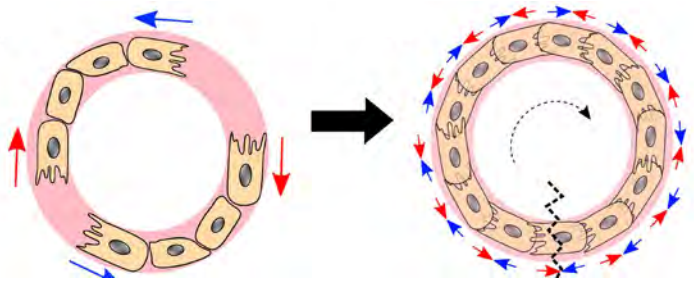

Flocking in 1D train, Jain, Ladoux & Mege, 2021

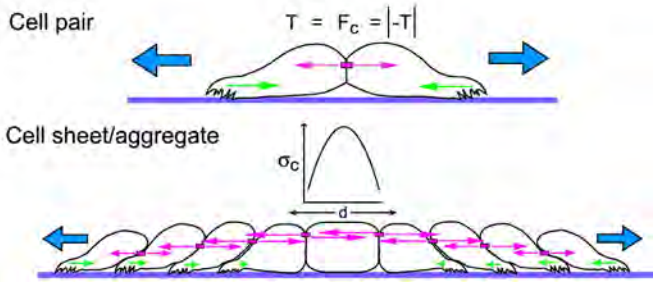

Collective cellular anti-alignement, Weber et al, 2012

Experimentally, different collective modes of motility **alignement or anti-alignement** in different cell types… or even in the same cell type as a function of **boundary conditions**

Theoretically, many of these interactions results in the same models of migration for infinite systems…

See also Veluda et al, 2012, Sepulveda et al, 2013, Basan et al, 2013, Camley et al, 2014, Bertrand et al, 2020, Bruckner et al, 2021, Ron et al, 2023

Geometry-driven migration efficiency of minimal cell clusters

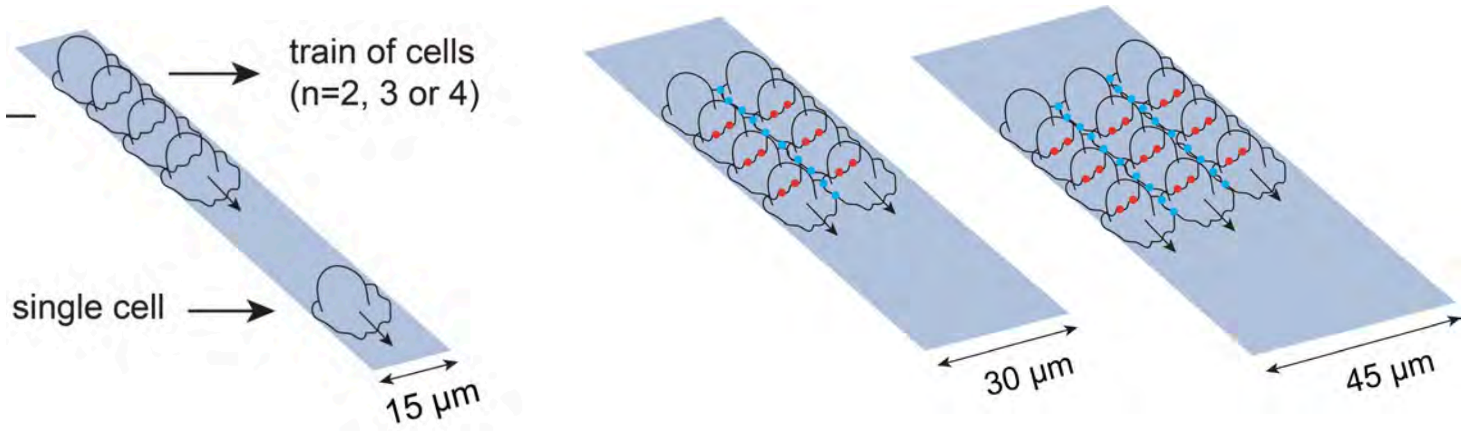

Eléonore Vercruysse

Sylvain Gabriele

Univ. Mons

David Bruckner
→ Biozentrum

How are collective modes of migration affected by varying boundary conditions in controlled ways?

Can we learn how active systems interact with each other by looking at how they react to boundaries?

Geometry-driven migration efficiency of minimal cell clusters

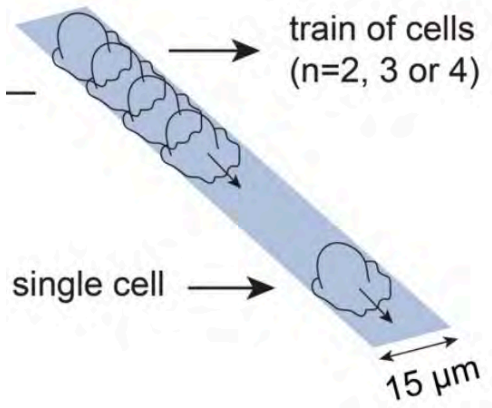

Fish keratocytes


Eléonore Vercruysse


Sylvain Gabriele


David Bruckner

Univ. Mons

How are collective modes of migration affected by varying boundary conditions in controlled ways?

Can we learn how active systems interact with each other by looking at how they react to boundaries?

Cell trains display length-independent migration speed…

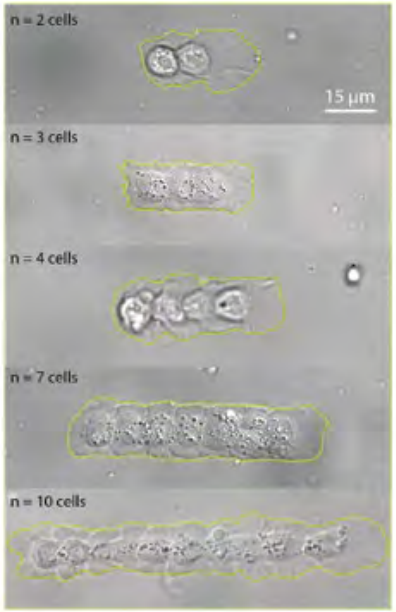

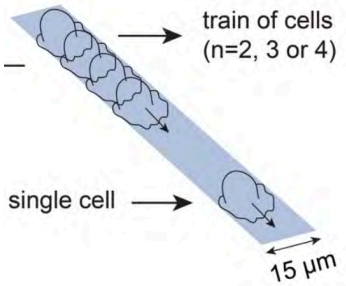

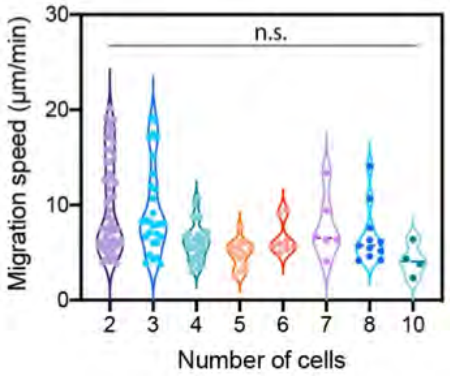

… but strongly width-dependent migration speed

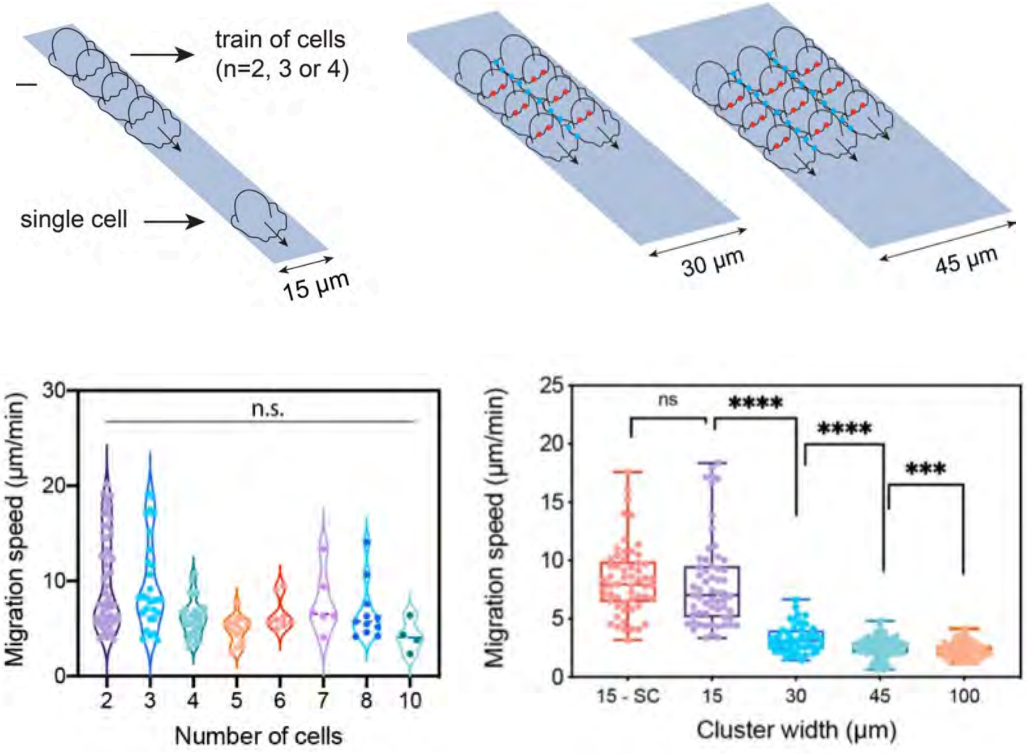

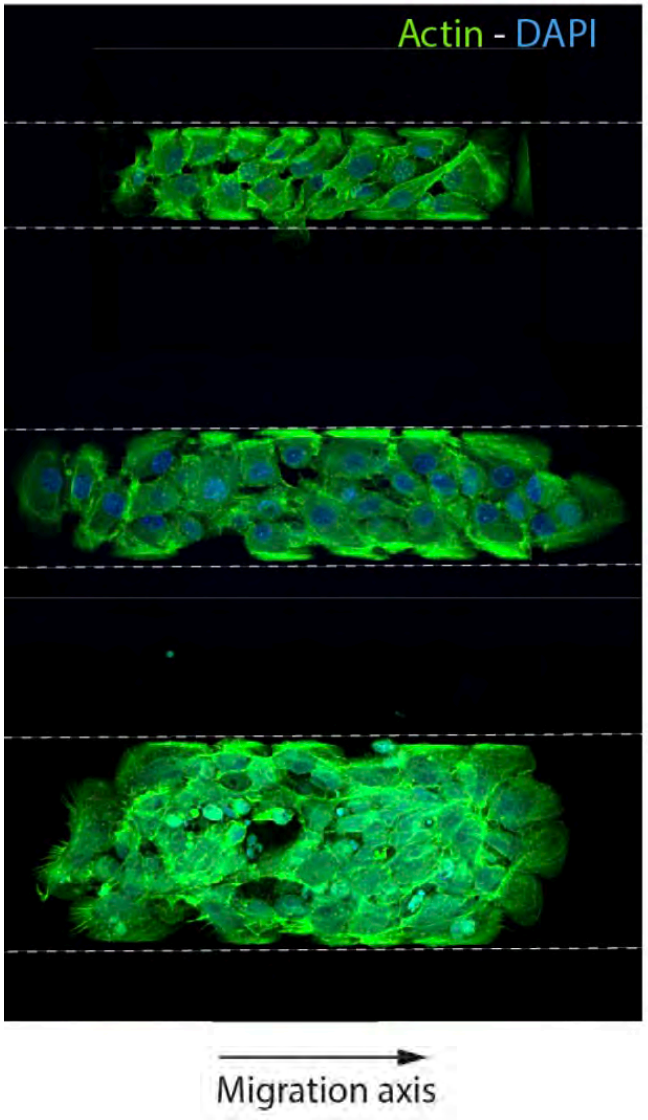

Systematically scanning cell-cell interactions based on symmetries

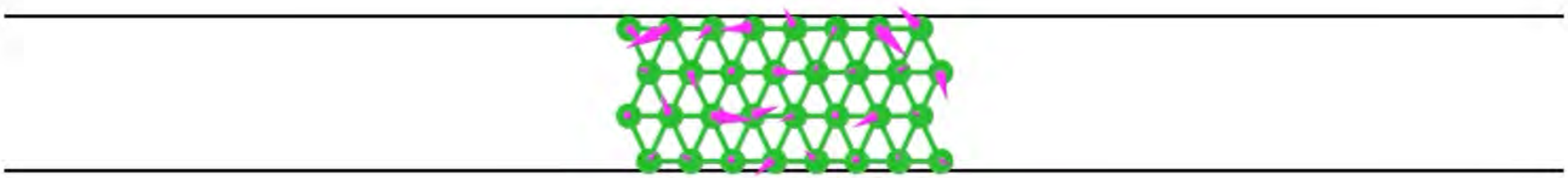

Cell trains as **elastically coupled, active interacting particles:**

$$\dot{\mathbf{x}}_i = k \sum_{j \in \mathrm{NN}} \mathbf{f}(\mathbf{x}_j - \mathbf{x}_i) + \mathbf{p}_i(t) - \nabla V_{\mathrm{confinement}}(\mathbf{x}_i)$$

Force balance

$$\dot{\mathbf{p}}_i = \mathbf{p}_i(1 - |\mathbf{p}_i|^2) + \mathbf{F}_i^{\mathrm{int}} + \sqrt{2D}\eta_i(t)$$

Polarity equation

Systematically scanning cell-cell interactions based on symmetries

velocity alignment (VA)

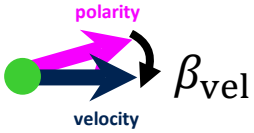

β_{vel}

$$\mathbf{F}_i^{\mathrm{int}} = \beta_{\mathrm{vel}} \dot{\mathbf{x}}_i$$

polarity alignment (PA)

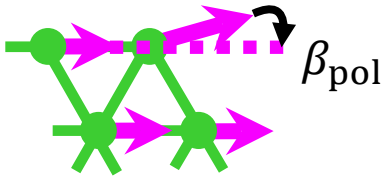

β_{pol}

$$\mathbf{F}_i^{\mathrm{int}} = \beta_{\mathrm{pol}} \left(\langle \mathbf{p}_j \rangle_{j \in \mathrm{NN}} - \mathbf{p}_i \right)$$

stress-polarity coupling (SPC)

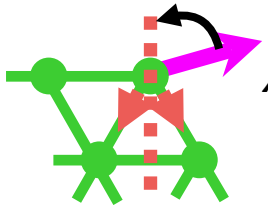

λ_{SPC}

$$\mathbf{F}_i^{\mathrm{int}} = -\lambda_{\mathrm{SPC}} k \sum_{j \in \mathrm{NN}} \mathbf{f}(\mathbf{x}_j - \mathbf{x}_i)$$

contact inhibition of locomotion (CIL)

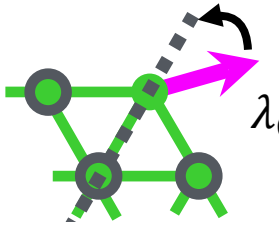

λ_{CIL}

$$\mathbf{F}_i^{\mathrm{int}} = -\lambda_{\mathrm{CIL}} \sum_{j \in \mathrm{NN}} \frac{\mathbf{x}_j - \mathbf{x}_i}{|\mathbf{x}_j - \mathbf{x}_i|}$$

$$\dot{\mathbf{p}}_i = \mathbf{p}_i (1 - |\mathbf{p}_i|^2) + \mathbf{F}_i^{\mathrm{int}} + \sqrt{2D}\eta_i(t)$$

Polarity equation

Systematically scanning cell-cell interactions based on symmetries

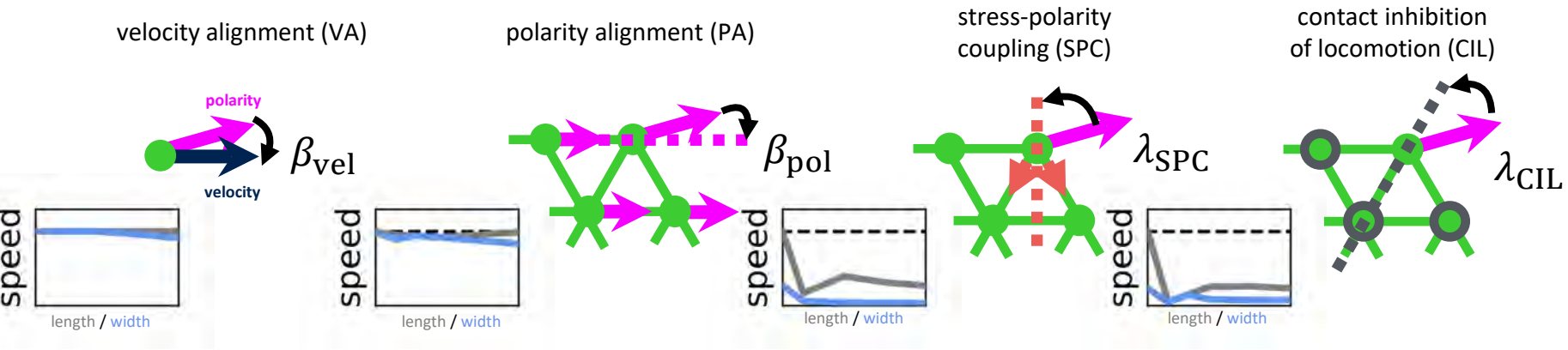

All models fail at recapitulating the data!

→ either always flock at the same speed regardless of width, or gets completely stuck by anti-aligments…

Even pair-wise combinations of models fail in all parameter regimes!

# Combining three interactions with nearly equal contributions recapitulates observations

velocity alignment (VA)

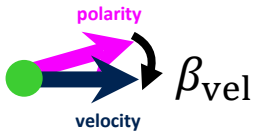

polarity alignment (PA)

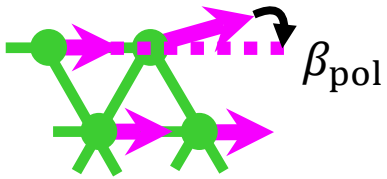

stress-polarity coupling (SPC)

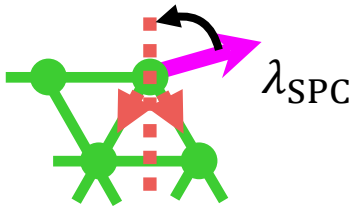

contact inhibition of locomotion (CIL)

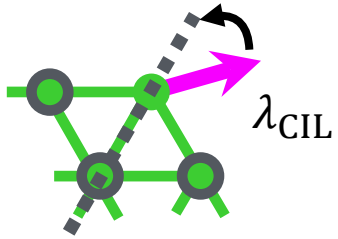

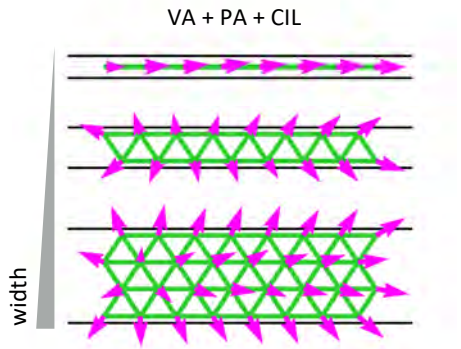

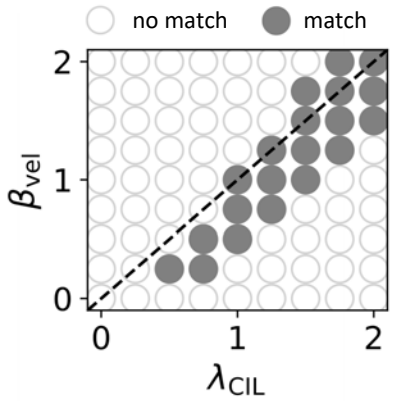

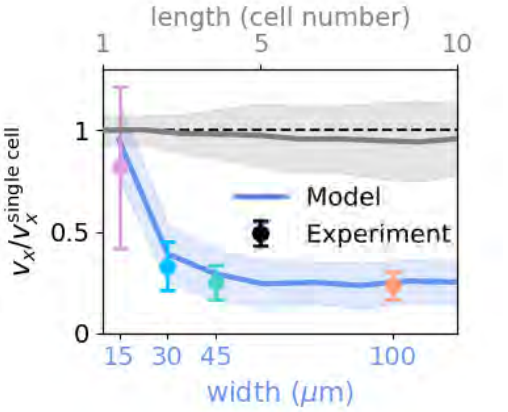

Velocity alignment guarantees global flocking…

Contact inhibition of locomotion creates outwards, unproductive polarization

Polarity alignment “propagates” this outward polarization inwards

# Combining three interactions with nearly equal contributions recapitulates observations

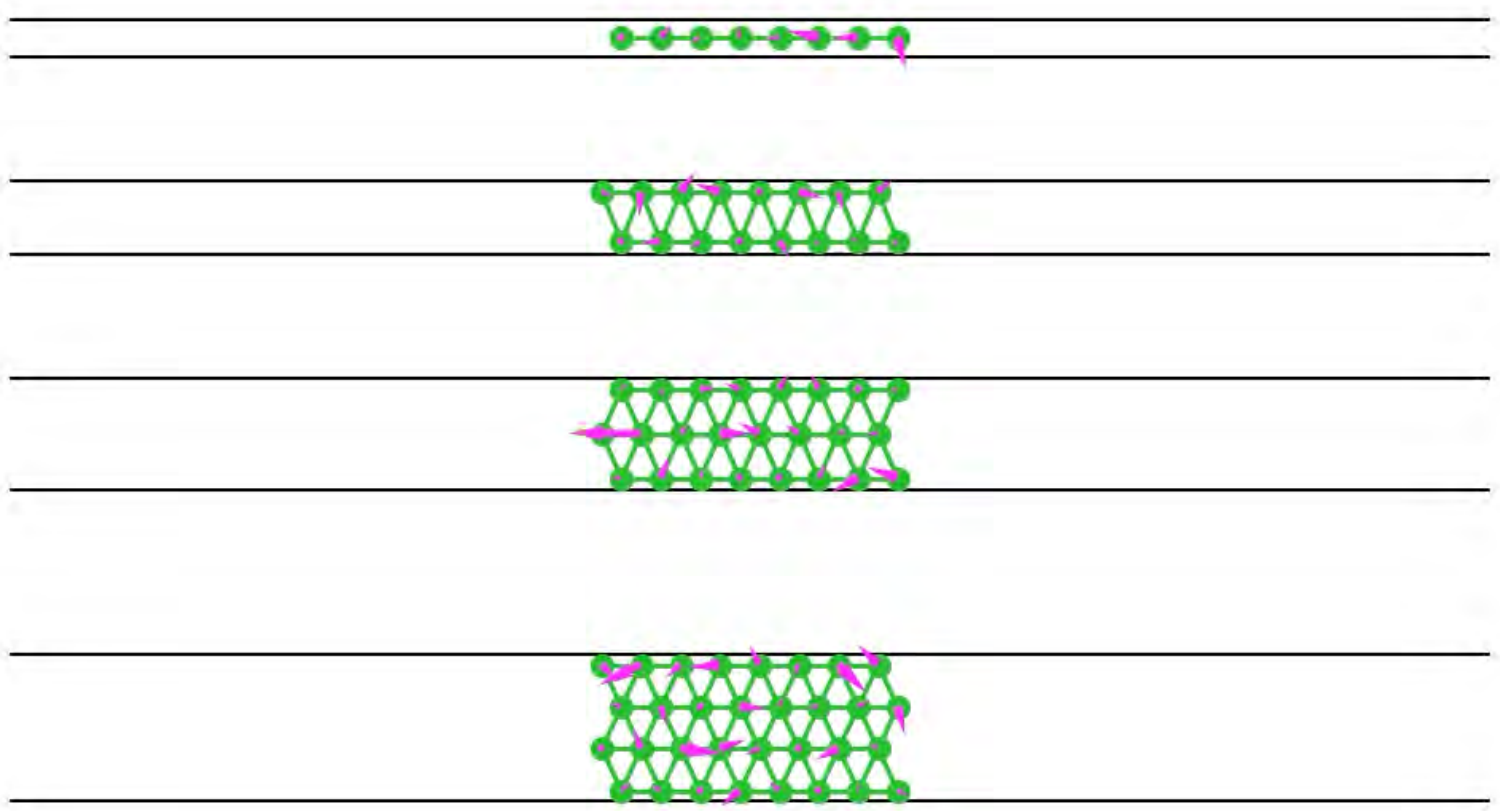

Model prediction: monolayer stress build-up in the orthogonal direction

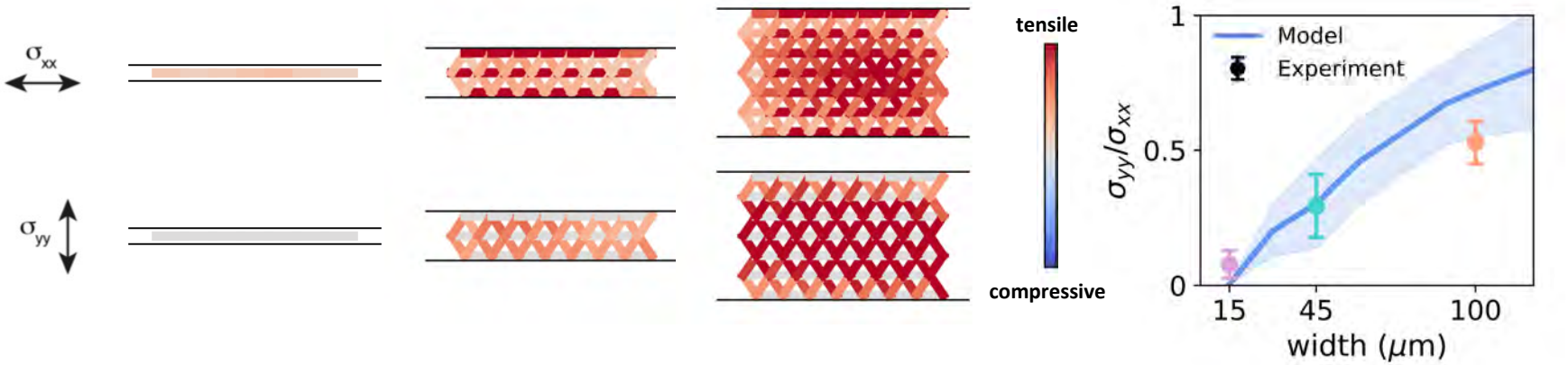

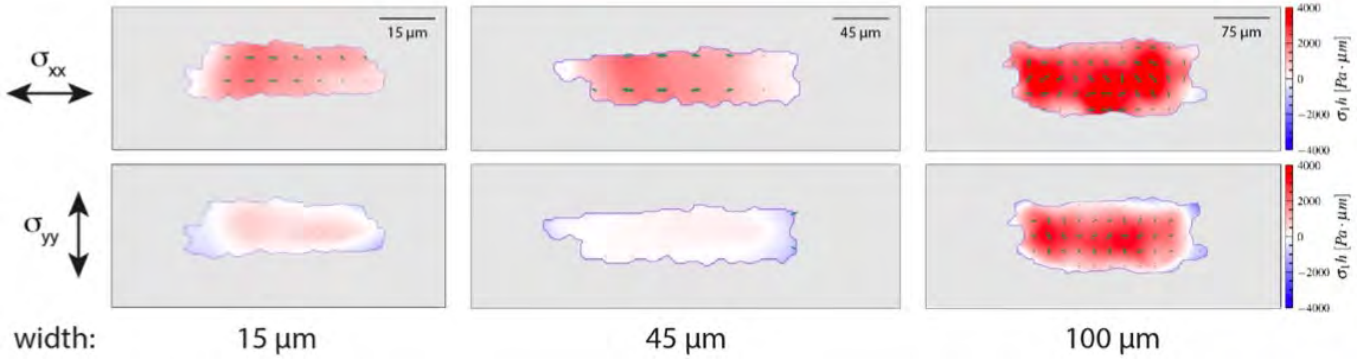

With M Gomez & X. Trepat, IBEC

Seemingly wasteful mechanism…

Are there any advantages/trade-offs that might explain why this is used by cells?

Model prediction: VA + PA + CIL gives optimal run & reorientation behaviour

polarity alignment (PA)

velocity alignment (VA)

VA + contact inhibition of locomotion (CIL)

VA + PA + CIL (experimental phenotype)

Optimal behavior for all three parameters with near equal contribution … very close to the inferred best-fit region…

Vercruysse*, Brückner* et al *Nat Phys* (2024)

Experiment: cell trains reorient efficiently upon collisions/dead-ends

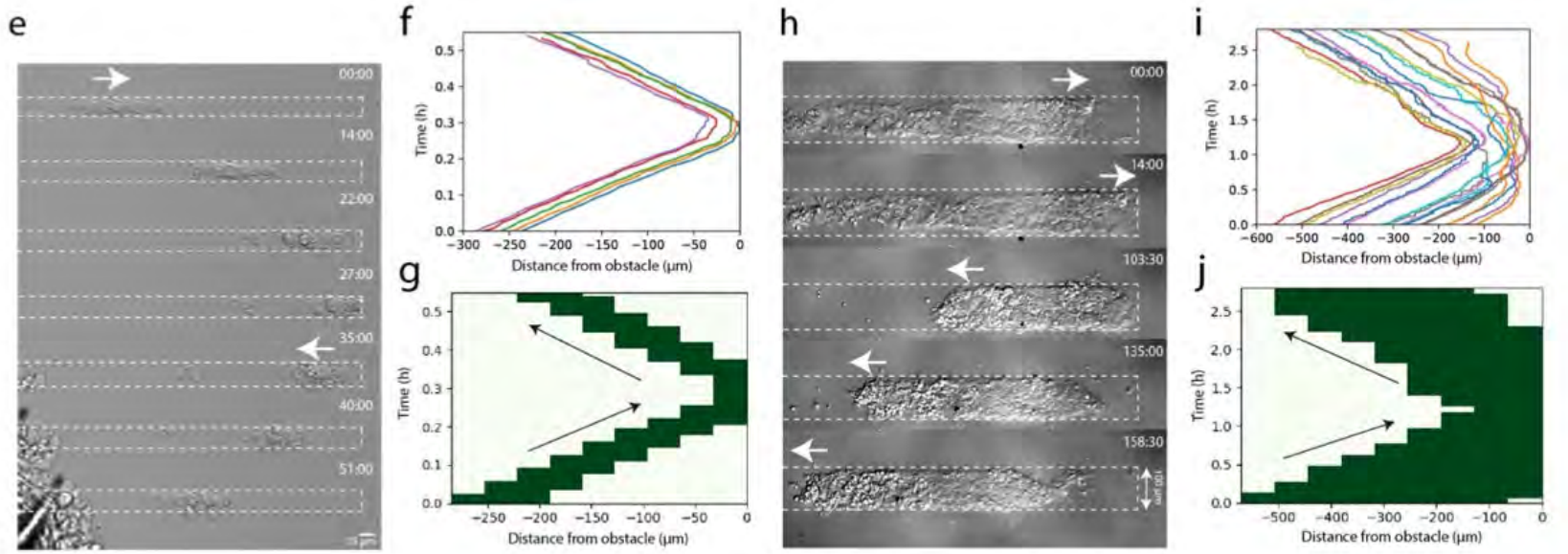

Nearly instantaneous collective repolarization regardless of width of the train!

Experiment: cell trains reorient efficiently upon collisions/dead-ends

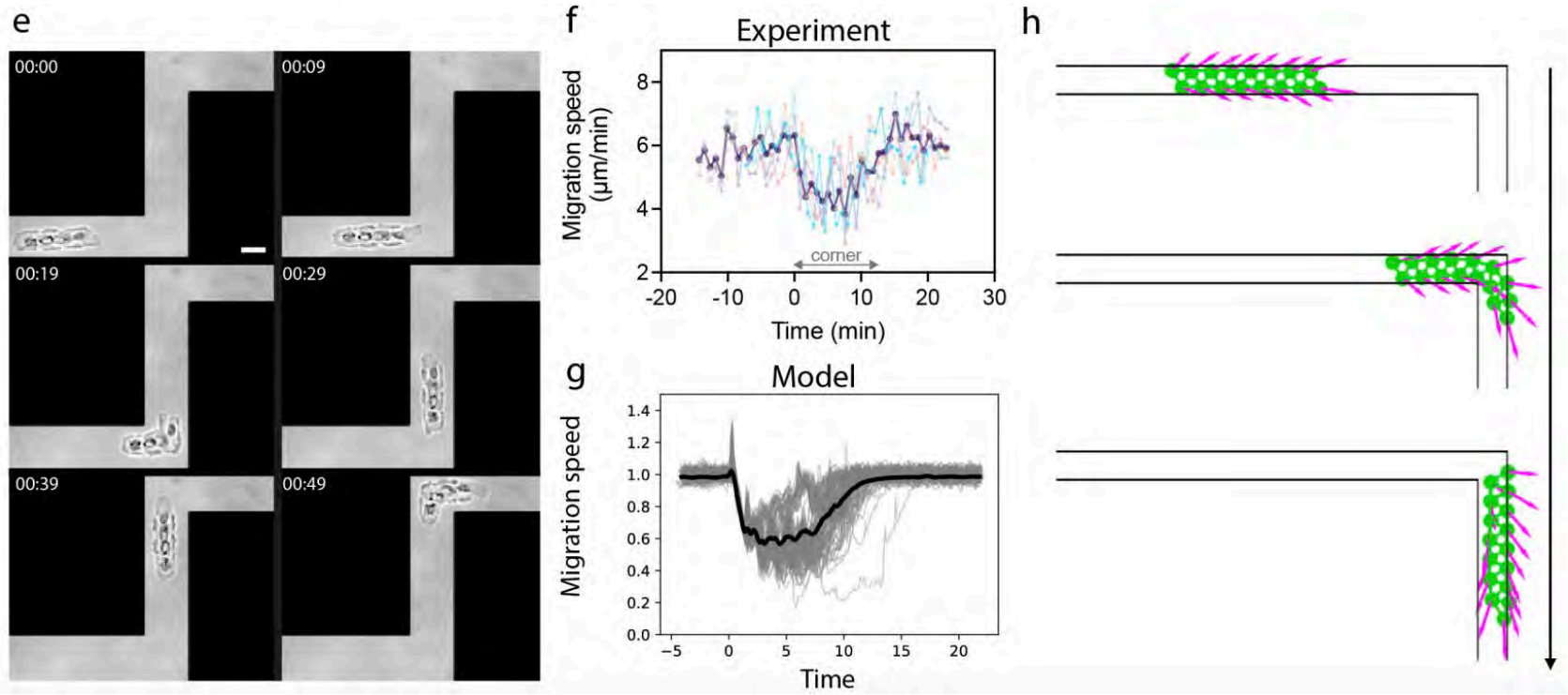

Nearly instantaneous collective repolarization regardless of width of the train!

Conclusion 2: Geometry-driven migration efficiency of minimal cell clusters

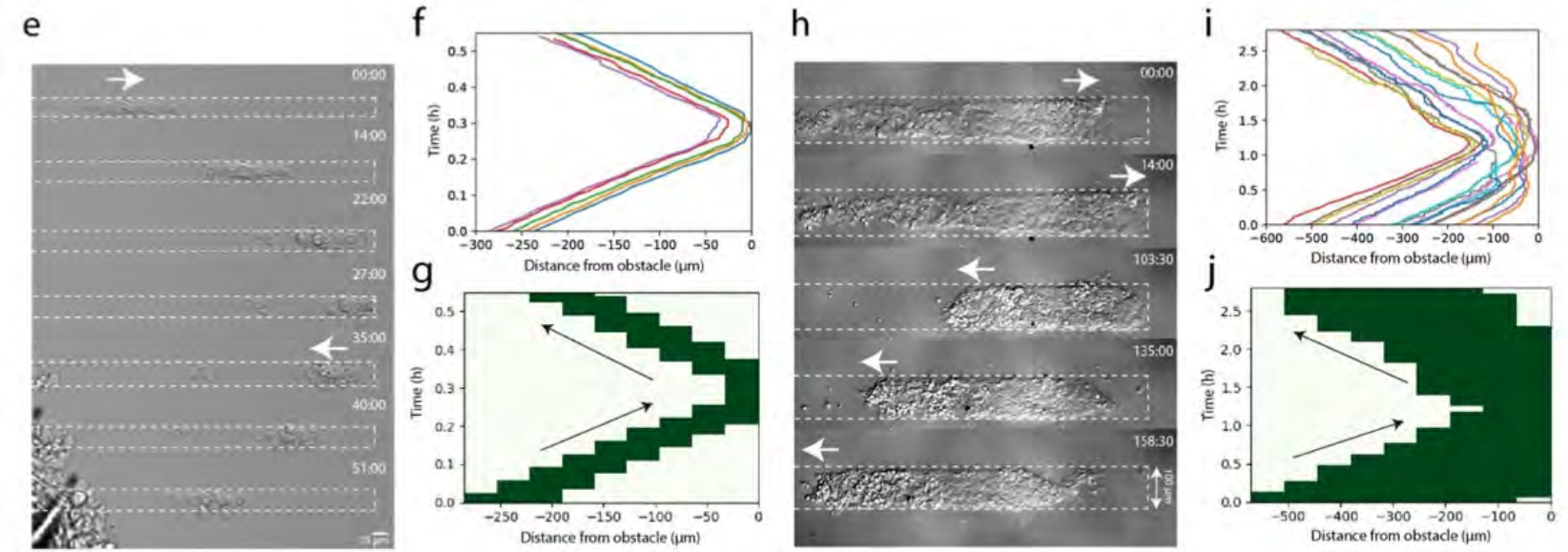

Importance of contact geometry in defining the migration properties of cell clusters.

Framework to extract interaction rules from how active systems interact with physical boundaries.

Vercruysse*, Brückner* et al *Nat Phys* (2024)

Part 3: Mechano-chemical instabilities and collective cell migration

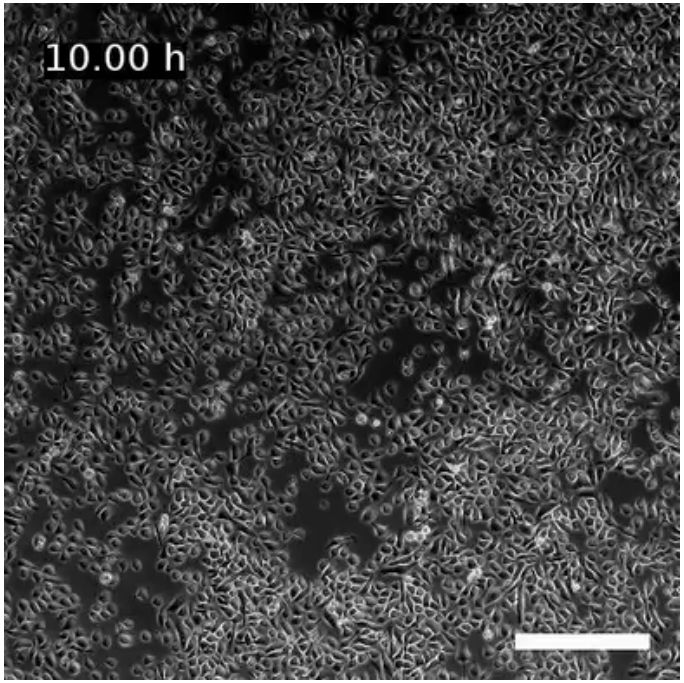

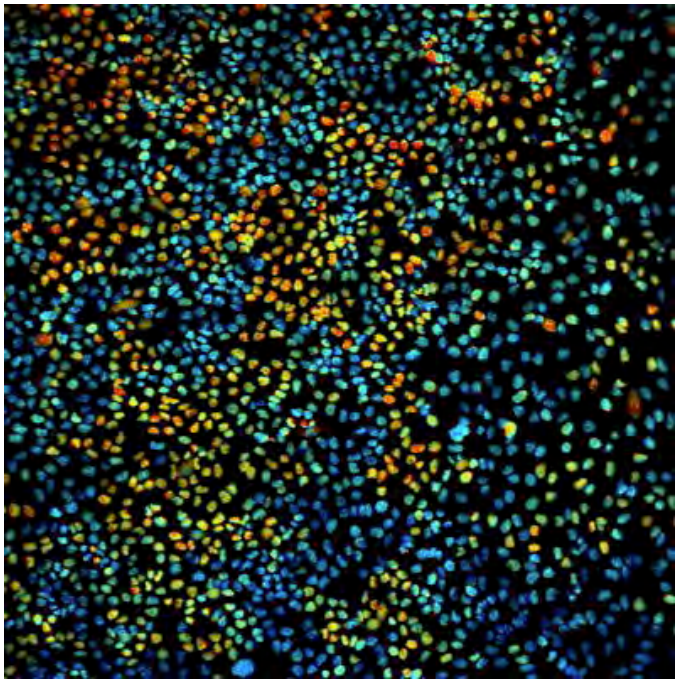

Quite a lot of active matter theories on this in the past decade (e.g. flocking, active glasses, zero-Reynolds turbulence etc)

… but limited information on the **internal/chemical state** of epithelial cells → can we really neglect these « hidden variables »?

E.g. Banerjee et al,, 2015, Blanc-Mercader et al, 2017, Notbohm et al, 2017, Tlili et al, 2018, Petroli et al, 2019, Henkes et al, 2020, Alert & Trepat, 2020

Mechano-chemical instabilities and collective cell migration

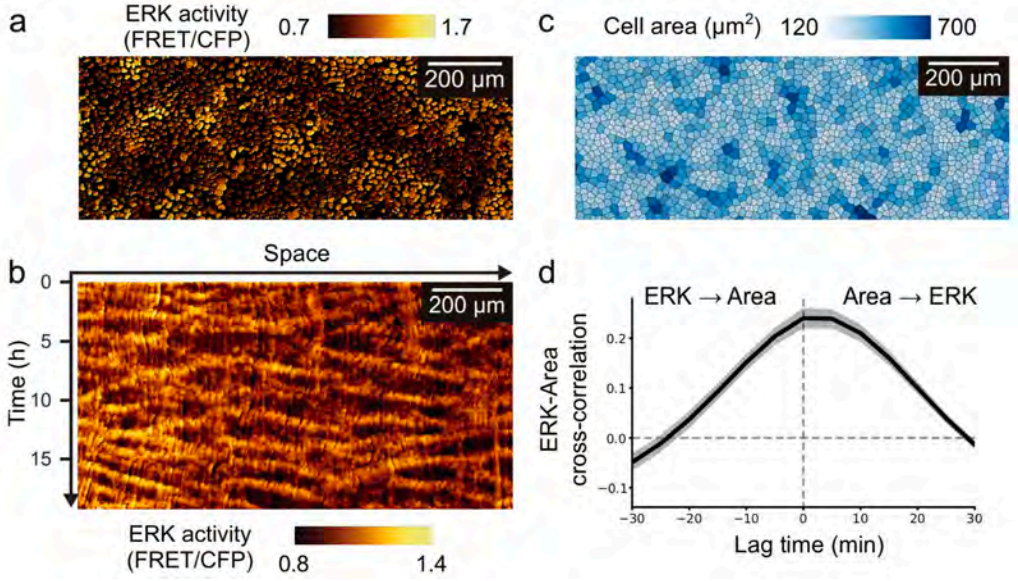

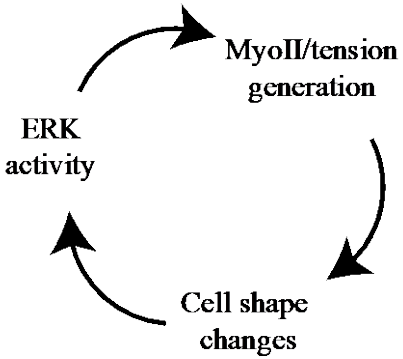

Daniel Boocock

Tsuyoshi Hirashima

Naoya Hino (→IST)

Kyoto University

Oscillations in space and time of both cell density and ERK signalling (with small delay).

Vertex-based models of tissues: tissues as active foams

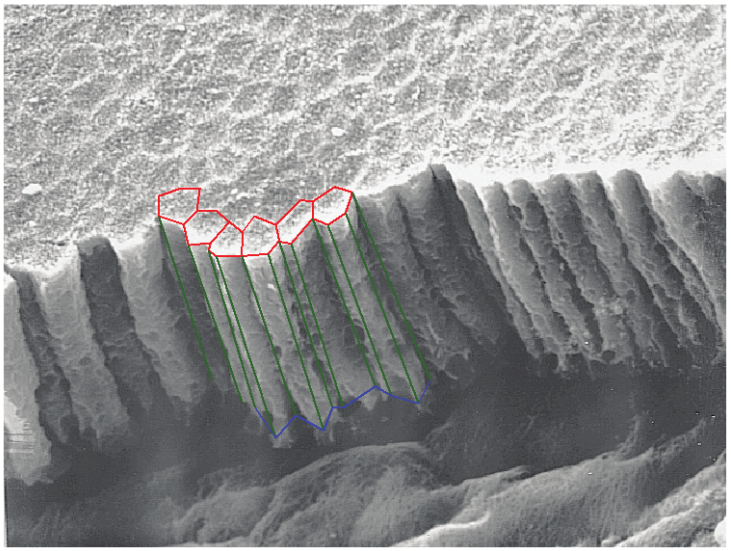

Epithelial tissues have a rather well-defined mesoscopic structure!
(apico-basal polarity, relatively ordered shapes, tight adhesion)

Equilibrium-like description: cell/tissue shape as a surface energy minimization process

From models of cells as active foams to collective oscillations

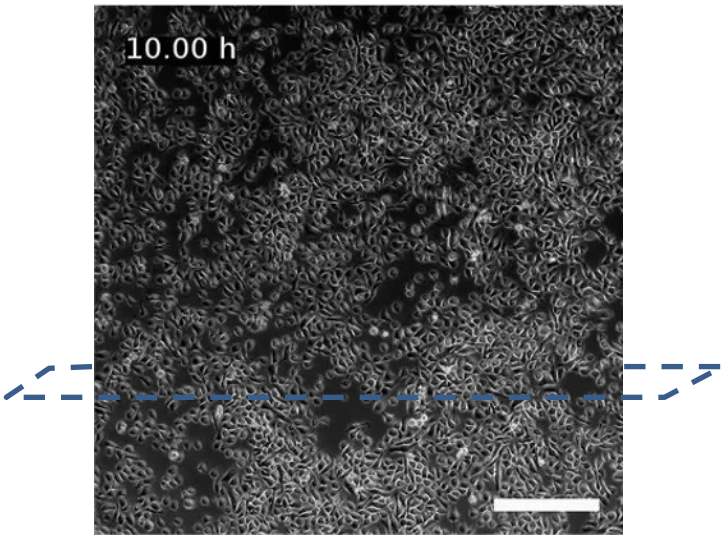

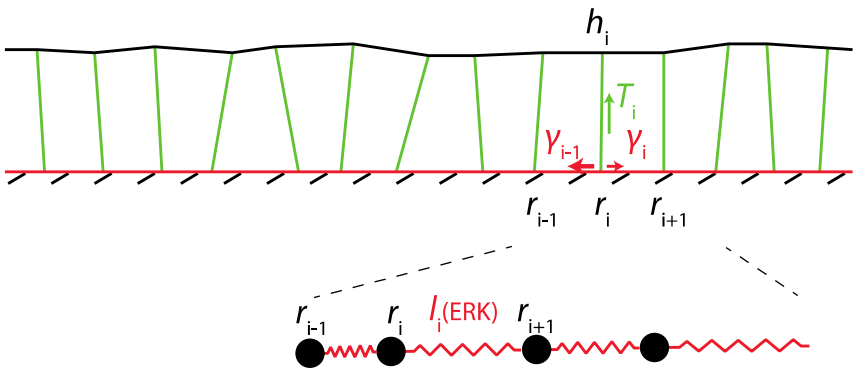

Cells as incompressible active foams under frictional contact with a substrate.

$$\mathcal{E}_i = T(ERK)h_i l_i + \gamma(ERK)l_i^2$$

Can be simplified to an overdamped chain of oscillators, and linearized as springs with rest length l_0 dependent on signalling (ERK) activity.

$$l_0 = \left(\frac{V_0}{2}\frac{T}{\gamma}\right)^{1/3}$$

Sign of coupling can be arbitrary as ERK can control differentially lateral, and apico/basal tensions.

Mechano-chemical model of ERK oscillations

$$\begin{cases} \tau_R \partial_t r = \partial_{xx} r - \partial_x l^0 \\ \tau_l \partial_t l_0 = -l_0 - \alpha E_r \\ \tau_E \partial_t E = -E + \beta \partial_x r \end{cases}$$

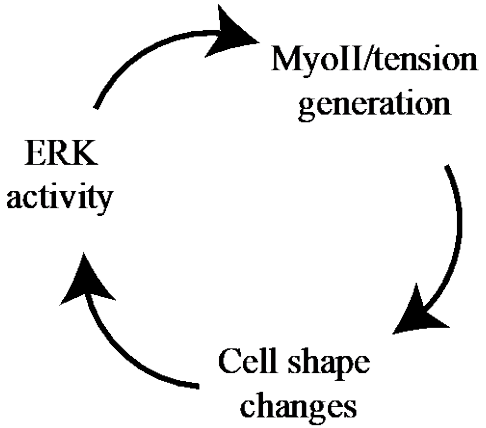

At linear order, this can be captured by three equations on:

- Cell position r (force balance)
- Cell rest length l_0 (dep. on ERK)
- ERK activity E (dep. on area)

→ Linearly unstable with a well-defined **spatial wavelength and temporal period**, for $\alpha\beta > \gamma(\tau_r, \tau_l, \tau_e)$

→ Isotropic mechano-chemical instability, depends only on the three timescales of the problem

Boocock*, Hino* et al, 2020

Testing the couplings between ERK and mechanics

Biochemistry → Mechanics

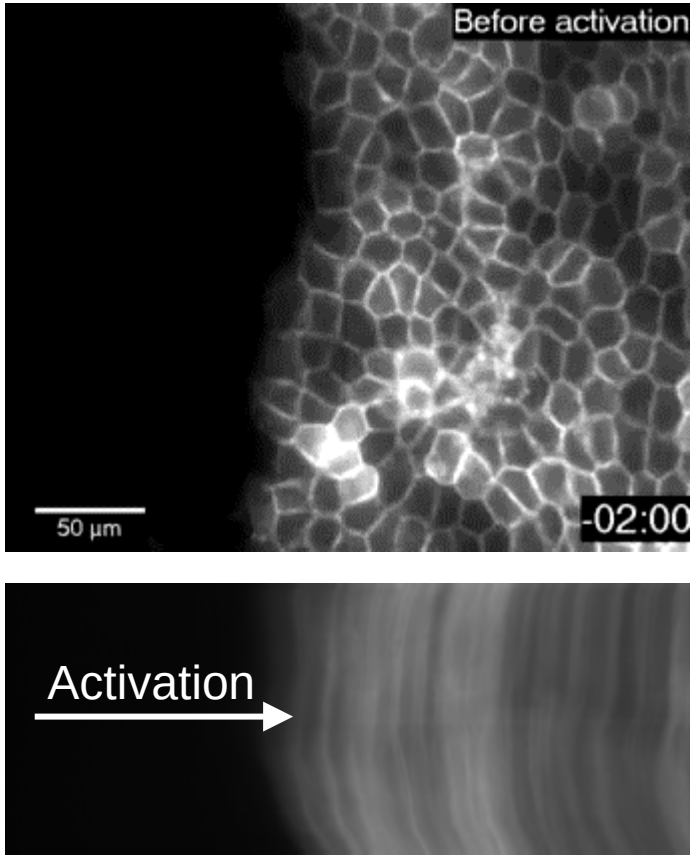

Optogenetically activating ERK decreases cell area

Mechanics → Biochemistry

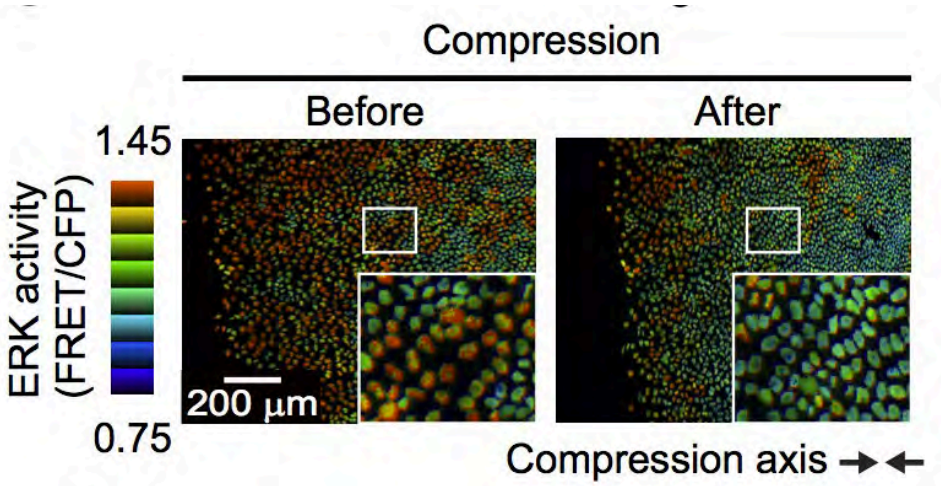

Decreasing cell area by compression **inhibits ERK** (and vice versa)

All parameters of the model extractable from these perturbations

Mechano-chemical patterns in confluent monolayers

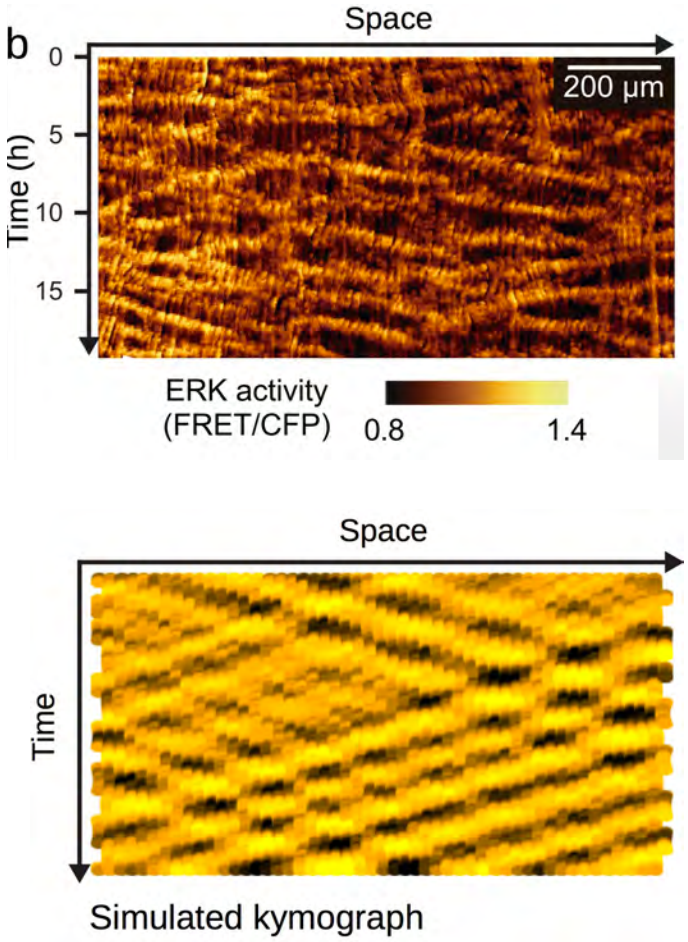

Parameter-free predictions match well the data:

$$\lambda = 2\pi \frac{\tau_E^{1/4} \tau_L^{1/4}}{\tau_R^{1/2}} \approx 10 - 20 \text{ cells}$$

$$T_{osc} = 2\pi \tau_l^{1/4} \tau_E^{3/4} \approx 55 - 105 min$$

What are these patterns good for?

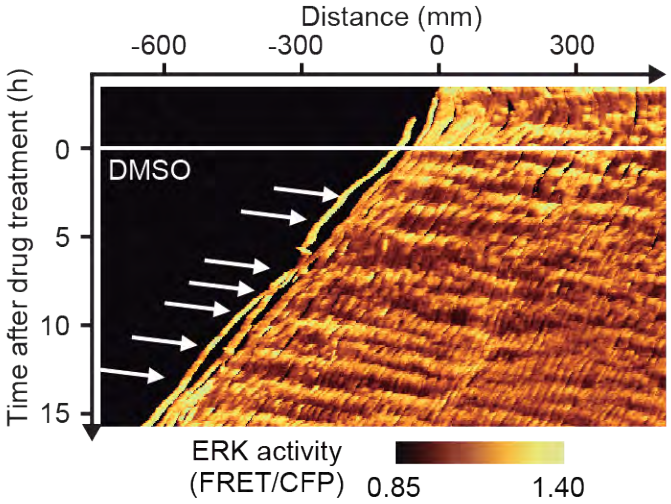

Symmetry-breaking: unidirectional ERK wave propagation during wound healing (also *in vivo* in mouse skin).

Accompanied by **long-range order** of migration polarity.

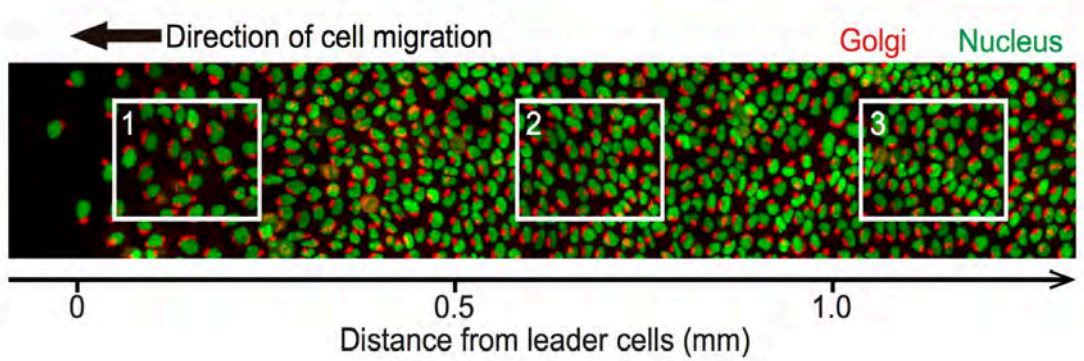

Hino et al, Dev Cell, 2020

What are these patterns good for?

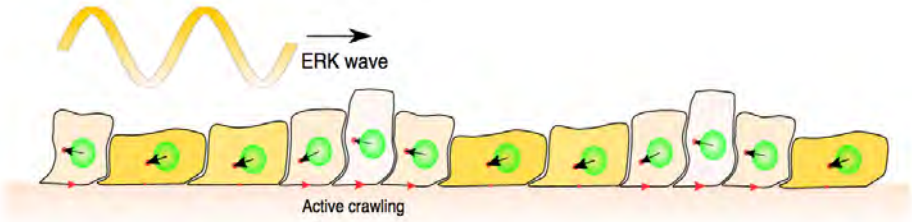

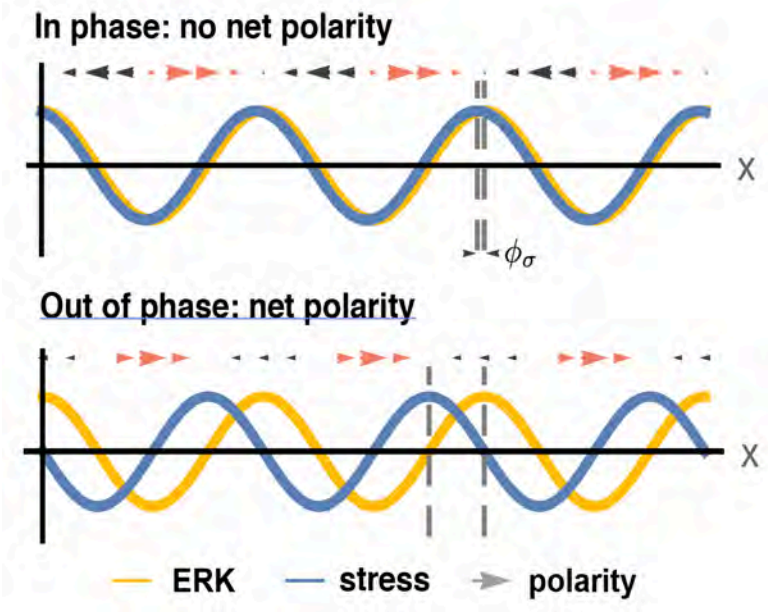

Coupling ERK-density mechano-chemical feedbacks with cell polarity ***p*.**

$$\tau_p \partial_t p = -p + D_p \partial_{xx} p + \gamma \partial_x \sigma_{xx}$$

Assumption of polarity coupled to gradients of stresses.

→**Not enough for symmetry breaking!**

(« back-of-the-wave paradox » in dictyostelium, see Levine, Goldstein, Murray, Sawai and many others)

Need for a non-linearity $\gamma(E)$**: becomes possible to exploit phase differences between chemical and mechanica waves:**

Direction of polarity from **gradient in mechanical stress**

Magnitude of traction forces from **chemical activity**

Response of a monolayer to an externally driven ERK wave

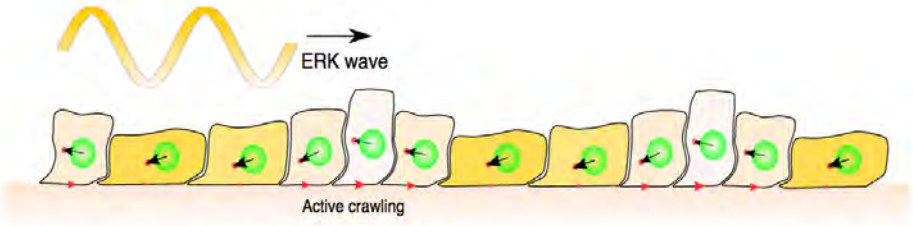

Only optimal for a unique value of pattern wavelength and period!

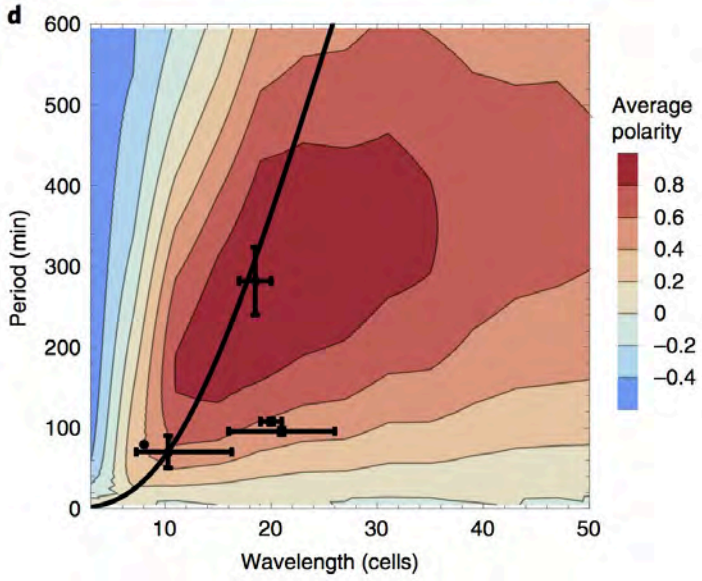

$$\overline{p}(\omega,k)=\lim_{\tau_p\to\infty}p(x,t|\omega,k)=\frac{1}{8\alpha}\frac{\omega k\left(\omega^2-k^2\right)}{\left(1+\omega^2\right)\left(k^4+\omega^2\right)}$$

Reported values are 1-6h and 10-30 cells (both *in vivo* and *in vitro*!)

Dispersion relation of the instability (black line) can only give rise to positive polarity → **robust polarization against a wave.**

Feedback between ERK wave directionality and long-range polarization

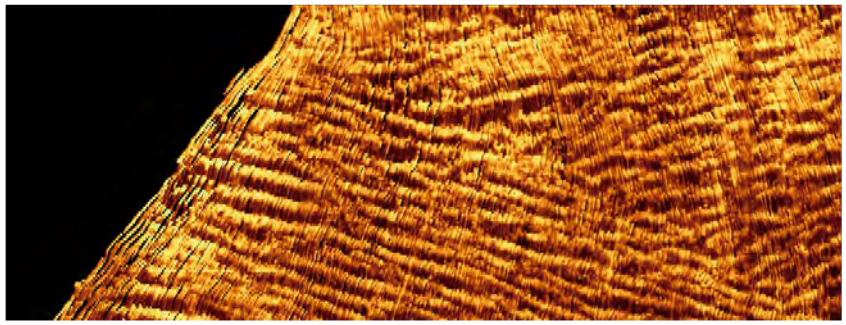

ERK

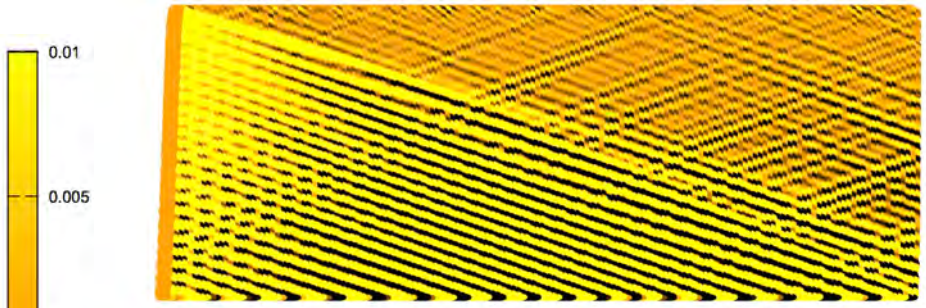

ERK

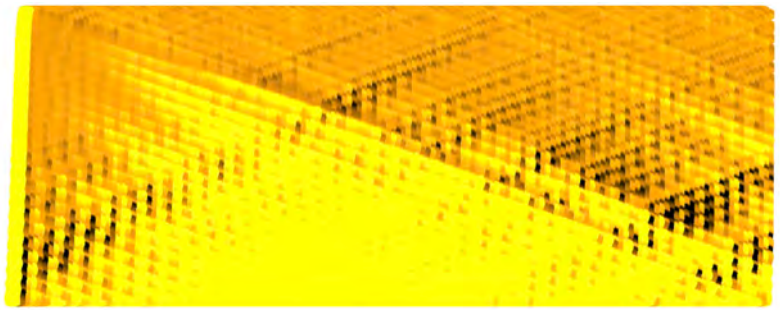

Polarity

Global polarization of ERK waves and polarity in response to a wound.

Model predicts the propagation of unidirectional ERK **waves away from the wound.**

Leads in return to long-range polarity towards the wound.

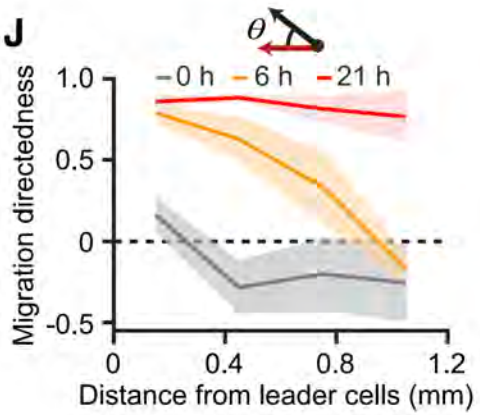

Hino et al, Dev Cell, 2020

Conclusion 3: From mechano-chemical waves to optimal monolayer polarization

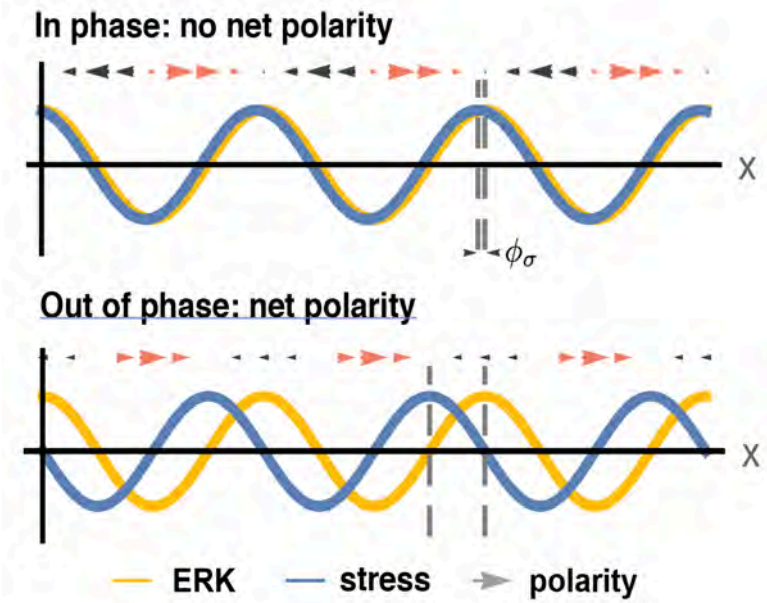

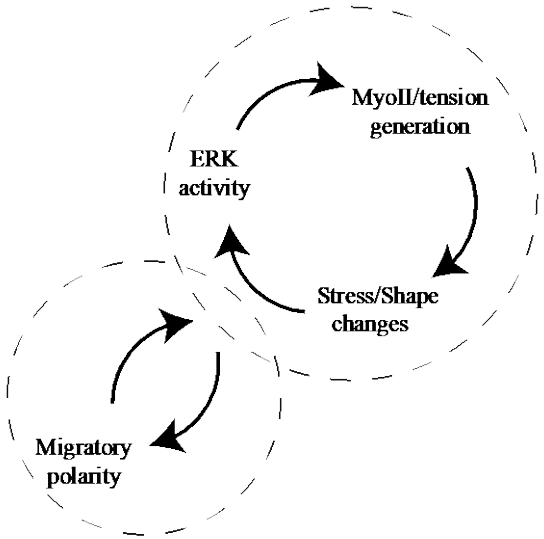

1. Density/ERK waves in monolayer as **an isotropic instability**, involving feedback delays between ERK and cell mechanics.

2. **Phase-shifts and non-linearities** in mechano-chemical waves allow for **symmetry-breaking and polarization.**

3. From biophysical origins to design principles of patterns: robustness and optimality for **long-ranged migration during wound healing**.

Boocock*, Hino* et al, Nat Phys, 2020

Mechano-chemical waves and defects in 2D

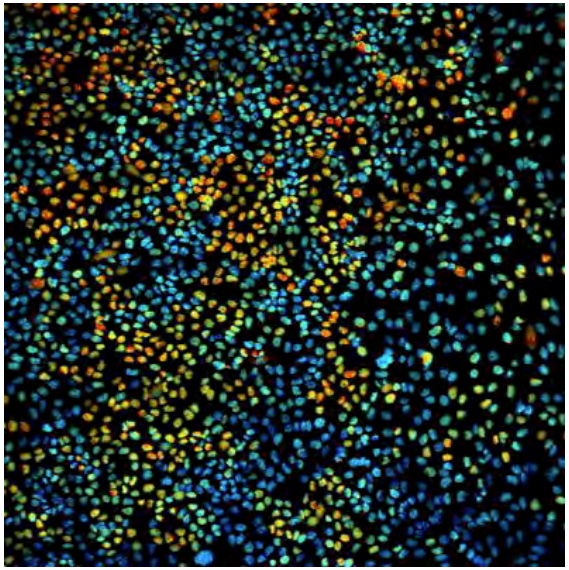

Mechano-chemical instabilities

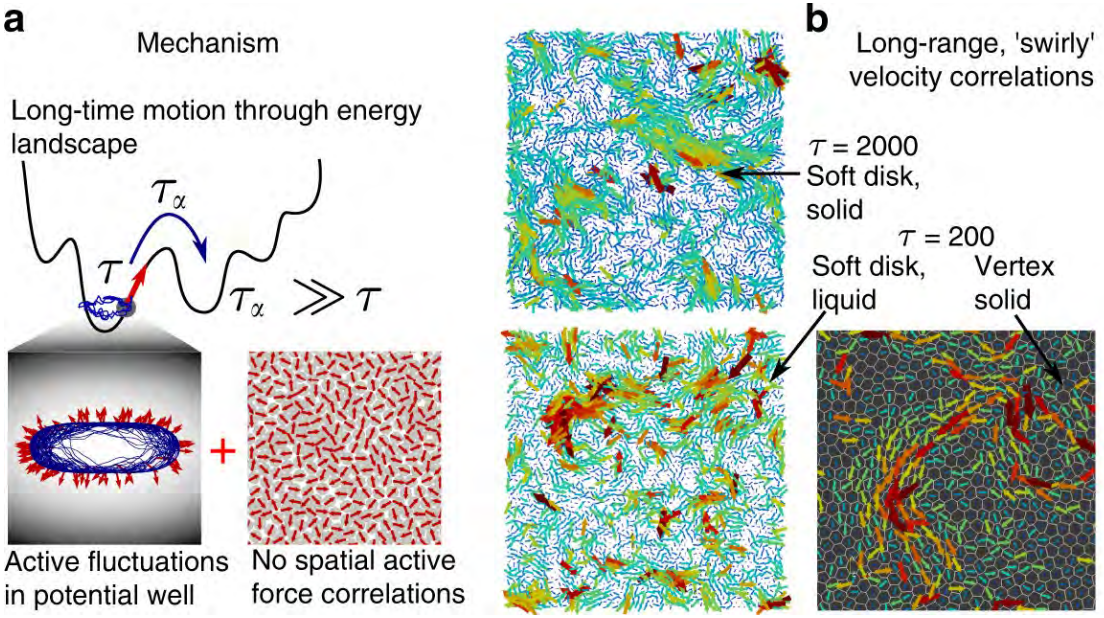

Glassy dynamics via active propulsion in an elastic sheet (Henkes et al, Nat Comm, 2020)

Unified description for the active 2D patterns formed by MDCK monolayers *in vitro*?

Generalizing our model to 2D

A - ERK-cell shape coupling

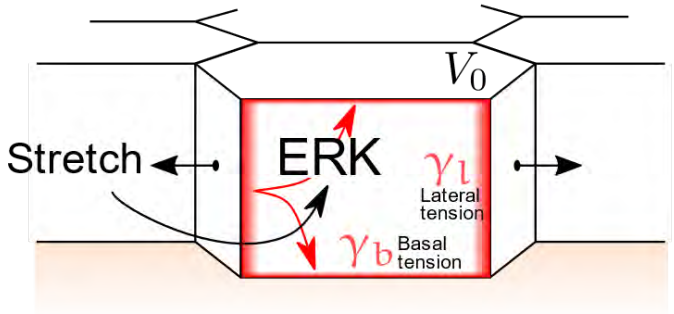

B - Model mechano-chemical couplings

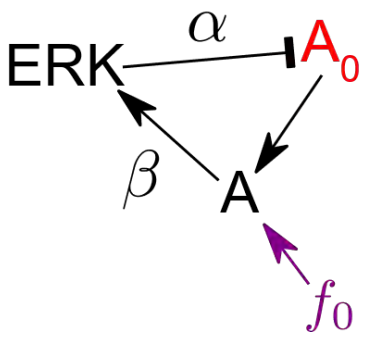

C - 2D vertex model and energy

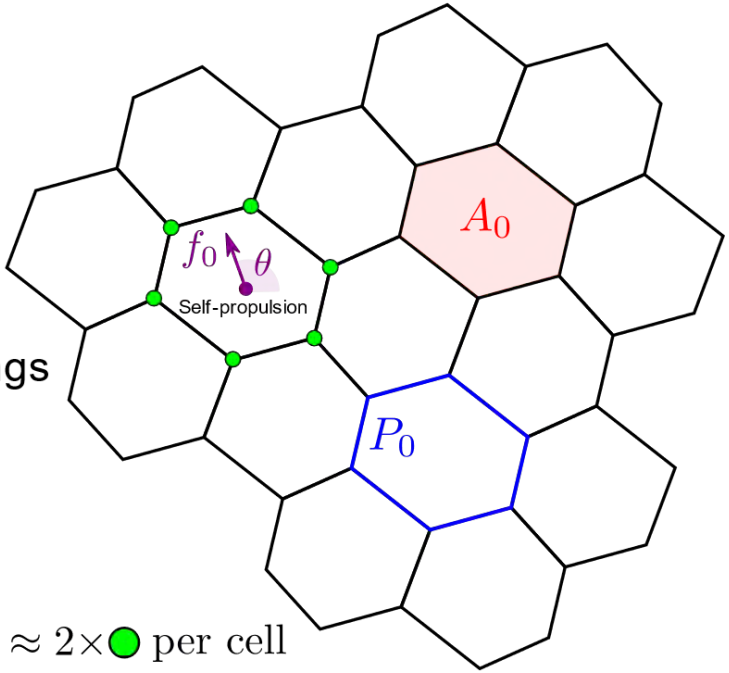

$\approx 2\times$ ● per cell

$$E = k_A(A - A_0)^2 + k_p(P - P_0)^2$$

Mechano-chemical equations + an active vertex model (Bi et al, PRX, 2016). Solid (resp. fluid) for low(resp high) shape index $p_0/\sqrt{A_0}$ (jamming) or for high enough active migration force f_0 (glass)

Transition from deterministic patterning to active glass

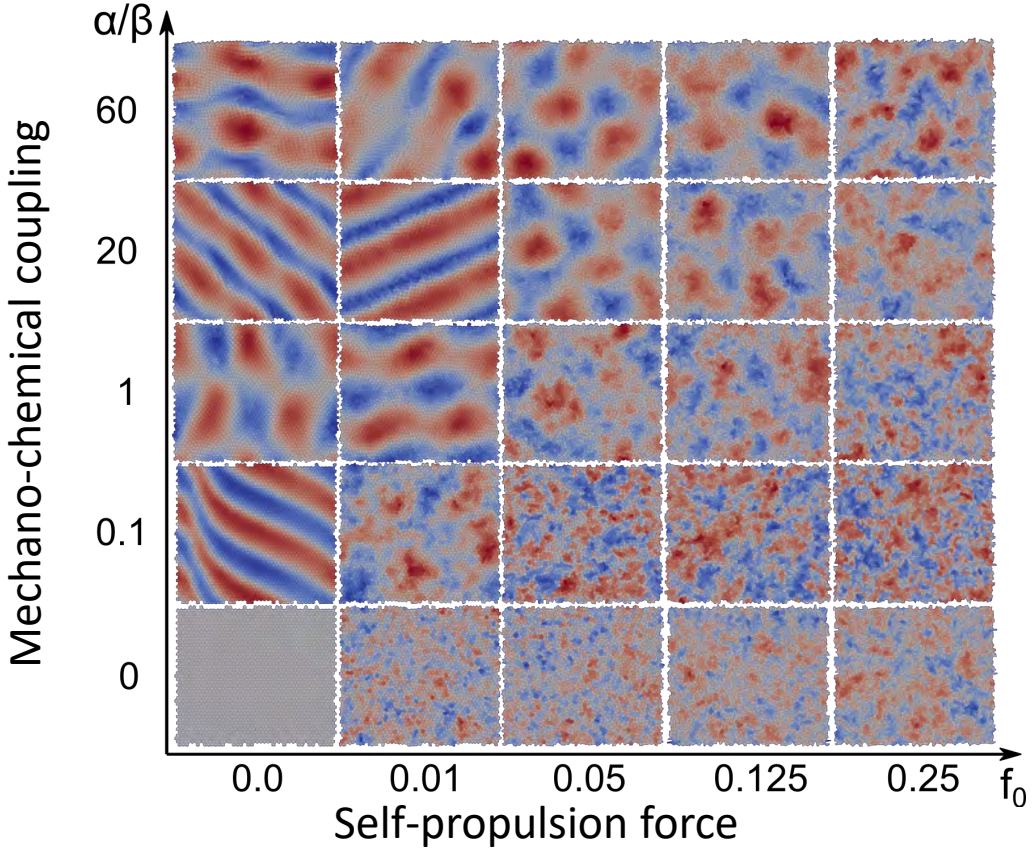

How can we constrain further parameters in this 2D description?

- α/β proportional to relative area vs ERK amplitudes
- $\alpha\beta$ and f_0 can be estimated from absolute amplitudes

Transition from deterministic patterning to active glass

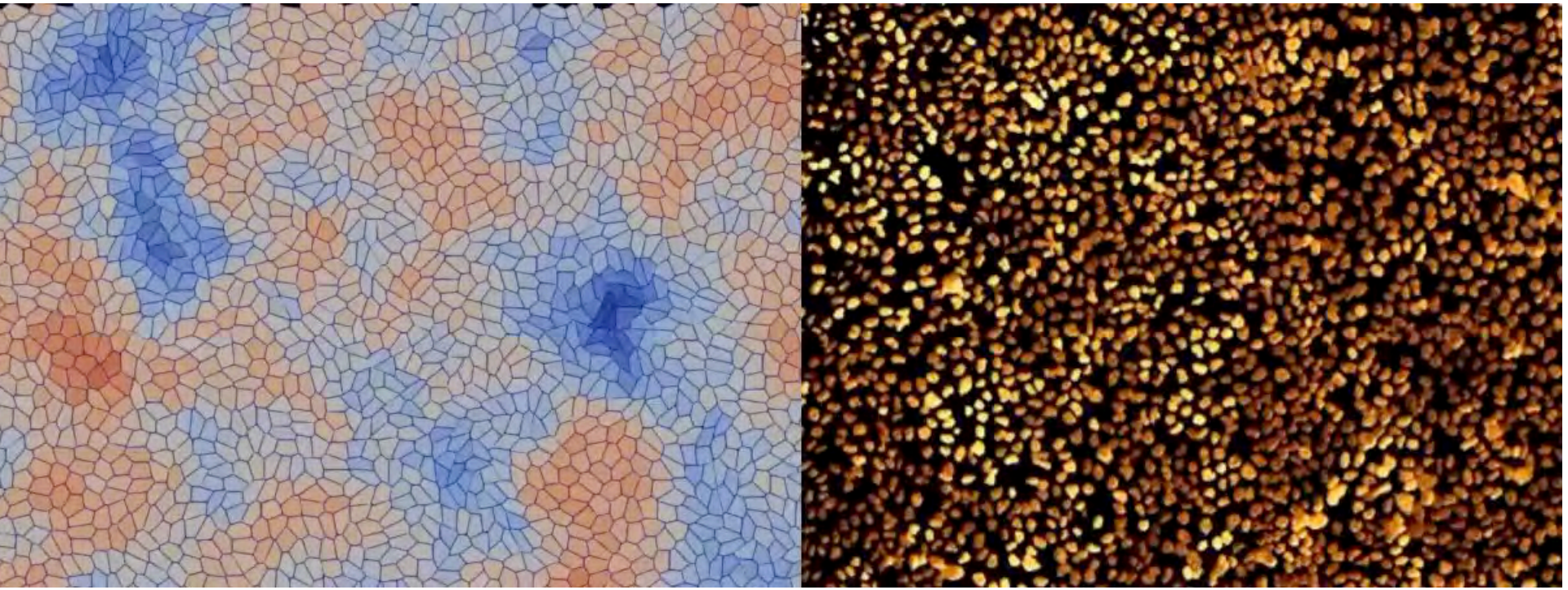

Boocock et al, 2023

Testing the model: how to quantify noisy 2D patterns?

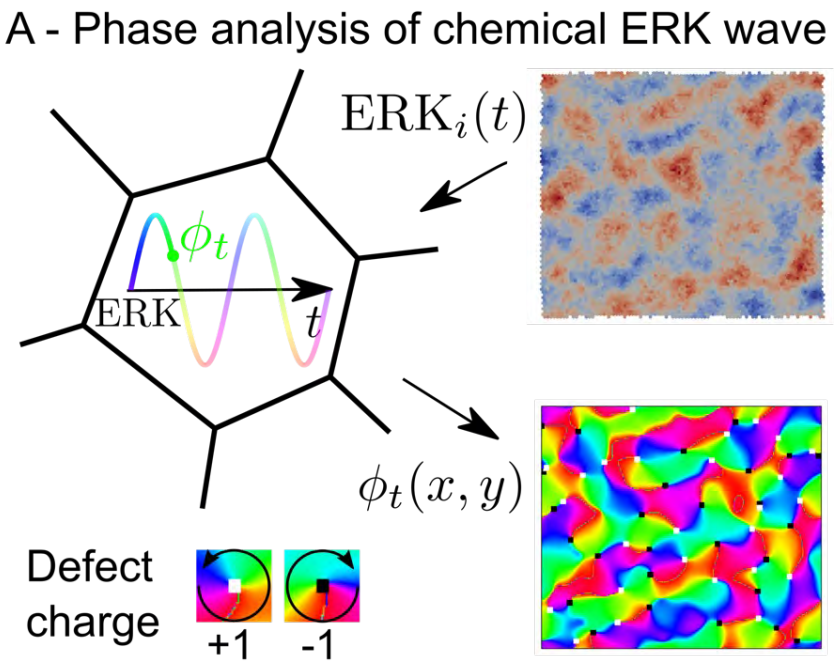

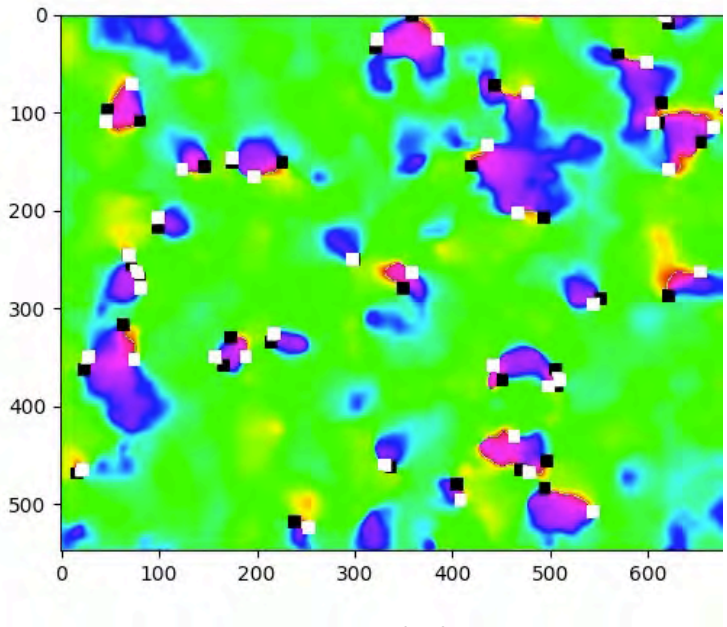

Experimental phase map
+ topological defects motion

Quantifying topological defects in the ERK phase field as a robust metric?
(see also Tan et al, Nat Phys, 2020)

Testing the model: how to quantify noisy 2D patterns?

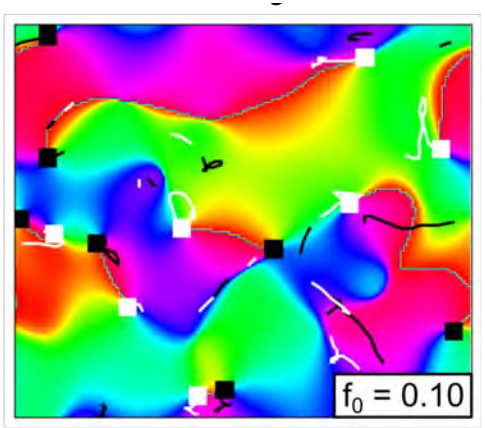

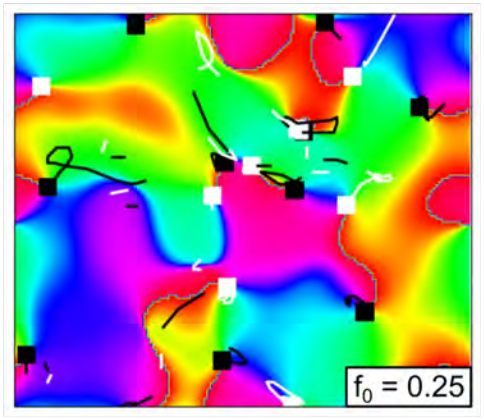

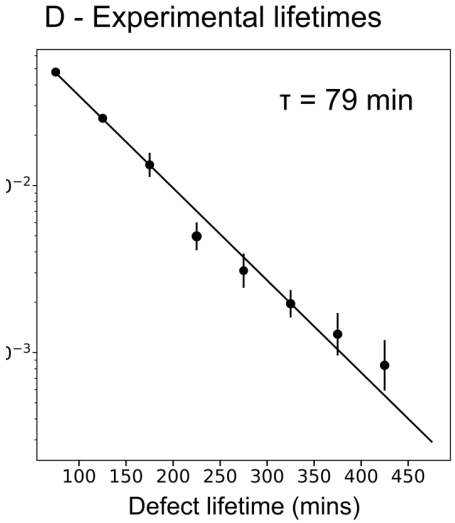

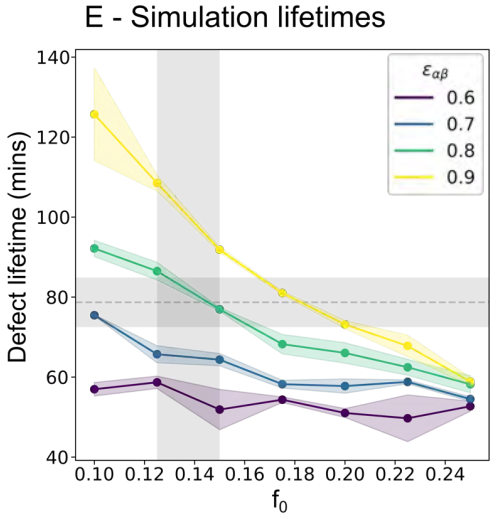

Already parametrized model can predict both the exponential distribution and average life time of defects.

Phase space in intermediary region between active glass and patterning!

Mechano-chemical phase controls local monolayer fluidization

A - Mapping ERK phase at T1 sites

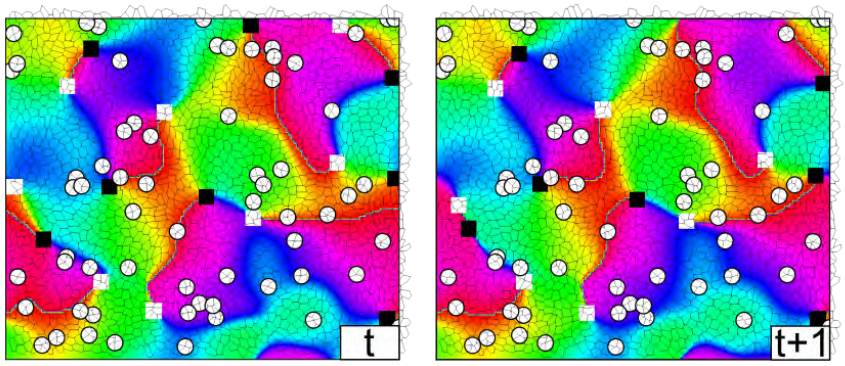

B - Distribution of ERK phase at T1 sites vs f_0

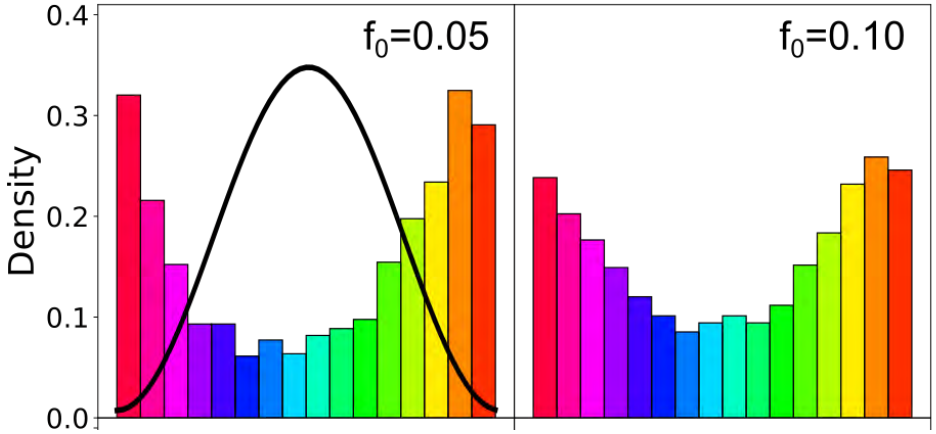

Mechano-chemical patterning amplitude $\alpha\beta$ only weakly affects overall T1 numbers (or MSD), i.e. **global material state**

But strong **local control** of T1 transitions in globally solid monolayers!

Spatio-temporal mechanism to control local tissue fluidity?

Outlook: Mechano-chemical models of complex tissue morphogenesis

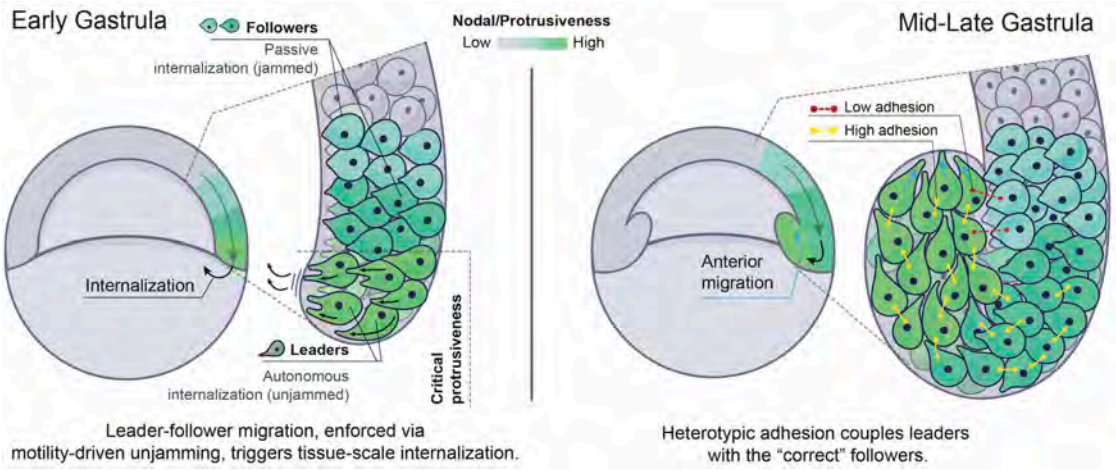

Pinheiro et al, Nat Phys, 2022

Integrating **morphogen gradients, migration and adhesion** in Zebrafish gastrulation

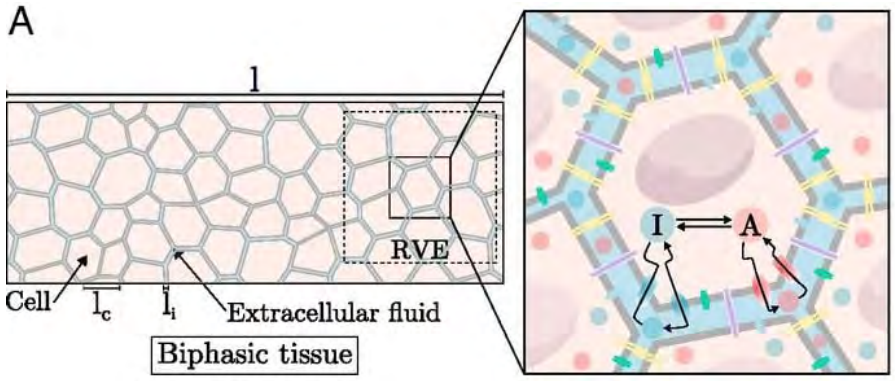

Recho et al, PNAS, 2019

Integrating **morphogen diffusion and tissue/fluid interactions**

Yang*, Xue, et al, NCB, 2021

Integrating **fate and mechano-osmotic forces** in intestinal organoids

Part 4: Collective cell migration in heterogeneous environments

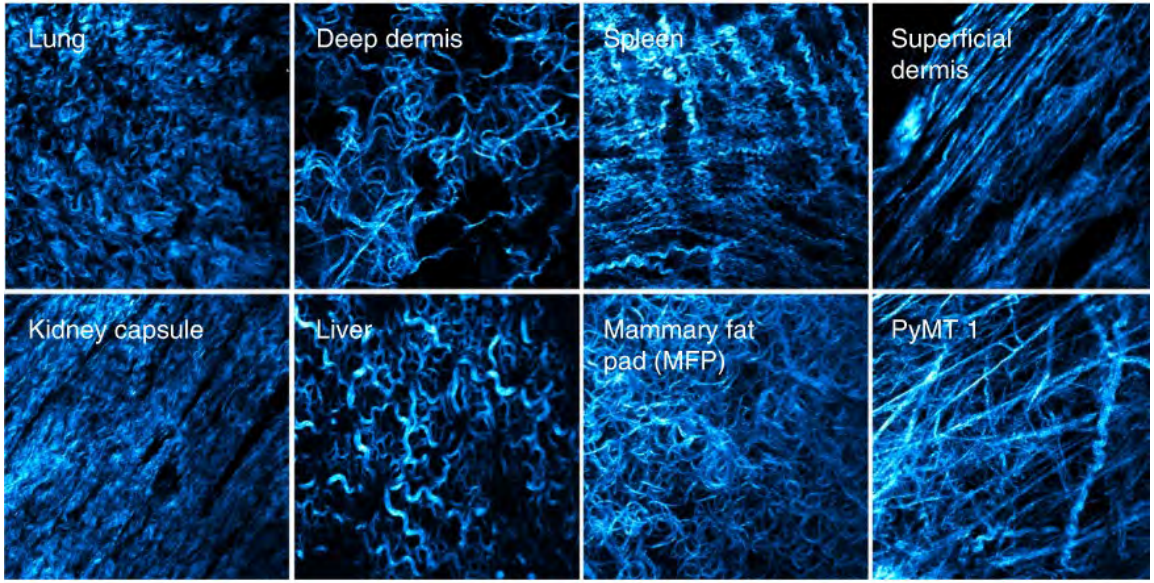

Park, D., et al. Nat. Mat (2020)

Collective migration *in vivo* typically occurs within a highly disordered environment…

Part 4: Environmental heterogeneity and tumor migration modes

Cell detachments as key step of cancer **metastasis**

Classical picture: lower adhesion (epithelial-mesenchymal transition)

Role of **mechanics** and **microenvironment**?

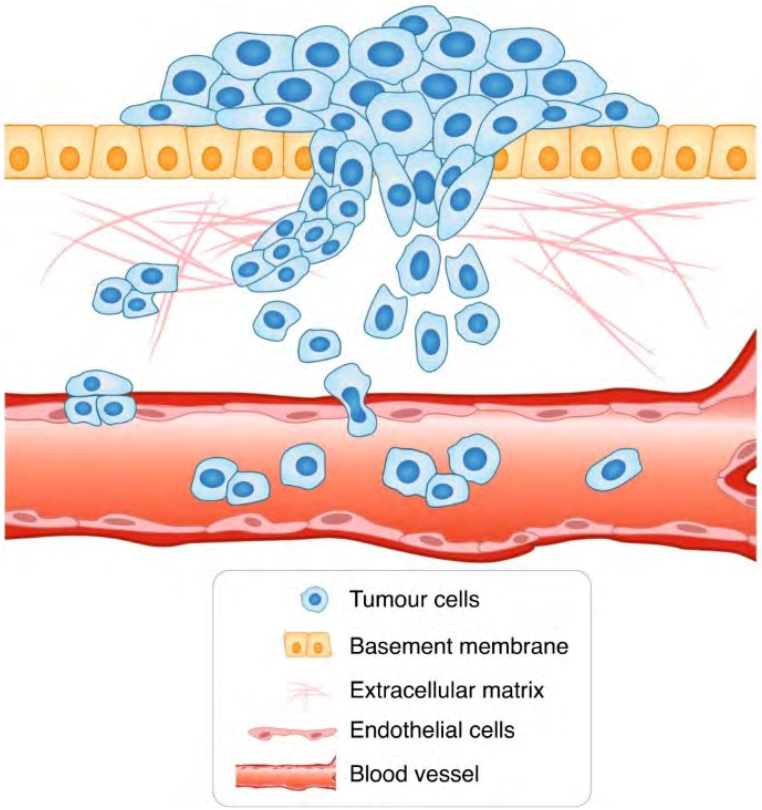

Adapted from: Novikov, N.M., *et al. Br J Cancer* (2021).

How does microenvironment geometry affect invasion collectivity?

Zuzana Dunajova

Saren Tasciyan

Michael Sixt

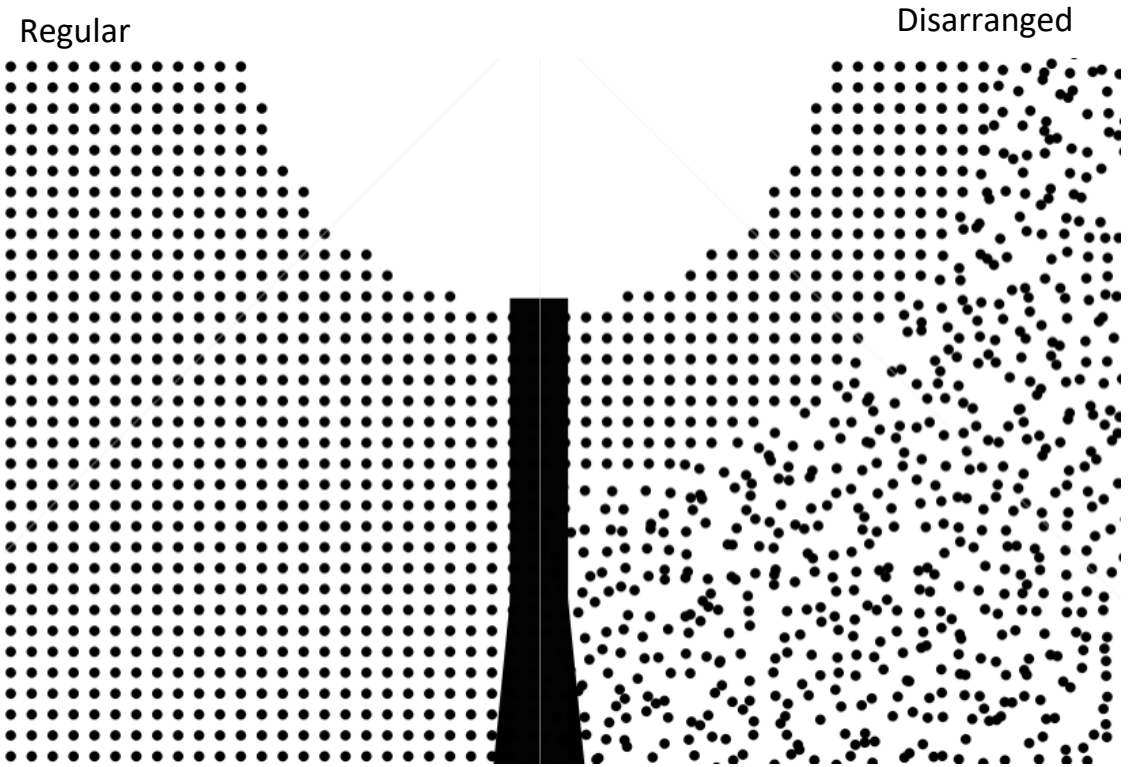

Controlled *in vitro* microfluidic experiments

Pillar patterns invaded by epidermoid carcinoma cells (A431)

See also Ilina et al, NCB, 2020, Kang et al, iScience, 2021

Detachments of cells induced by disordered environment

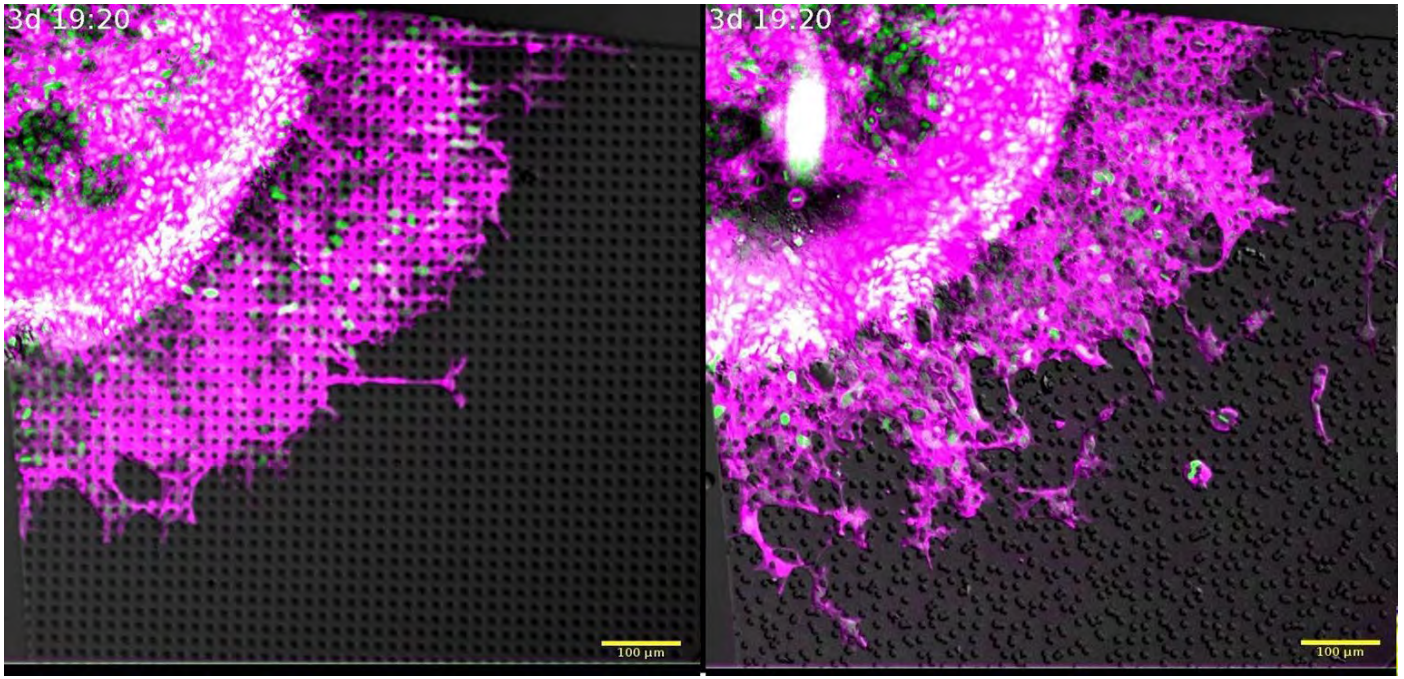

No obstacles at all → collective mode of migration without detachements…

Regular obstacles → collective mode of migration (irrespective of lengthscale)

Random obstacles → single-cell mode of migration, similar to E-P-Cadherin knockout!

Can we capture this behavior with a minimalistic model?

Biased active particles with attraction in a disordered medium

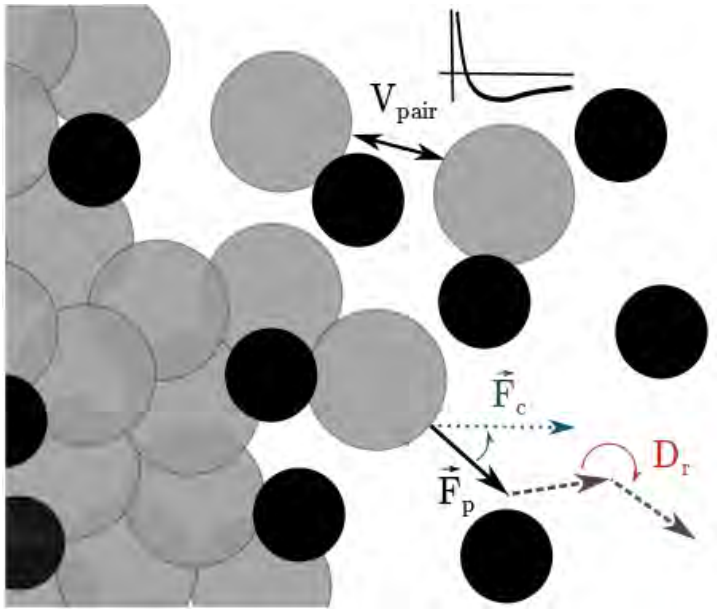

$$\gamma \frac{d\vec{x}}{dt} = \frac{dV_{\text{pair}}}{dr} + \vec{F}_{\text{p}}$$

$$\frac{d\theta}{dt} = -kcos(\theta) + \sqrt{2D_{\text{r}}}\eta$$

$$V_{\text{pair}}(r) = \begin{cases} 4\varepsilon \left[\left(\frac{\sigma}{r}\right)^4 - \left(\frac{\sigma}{r}\right)^2 \right] & \text{if } r < r_{\text{cut}} \\ 0 & \text{if } r \geq r_{\text{cut}} \end{cases}$$

γ - friction coefficient

$\vec{F}_p$- cellular self propulsion

D_r- rotational diffusion constant

η - unit variance random variable

ε - well depth

σ ~ cell size

J. A. Anderson, J. Glaser, and S. C. Glotzer. Comput. Mater. Sci. (2020)

Can we capture this behavior with a minimalistic model?

Very generic/robust feature: extensive cell detachments in disordered pattern

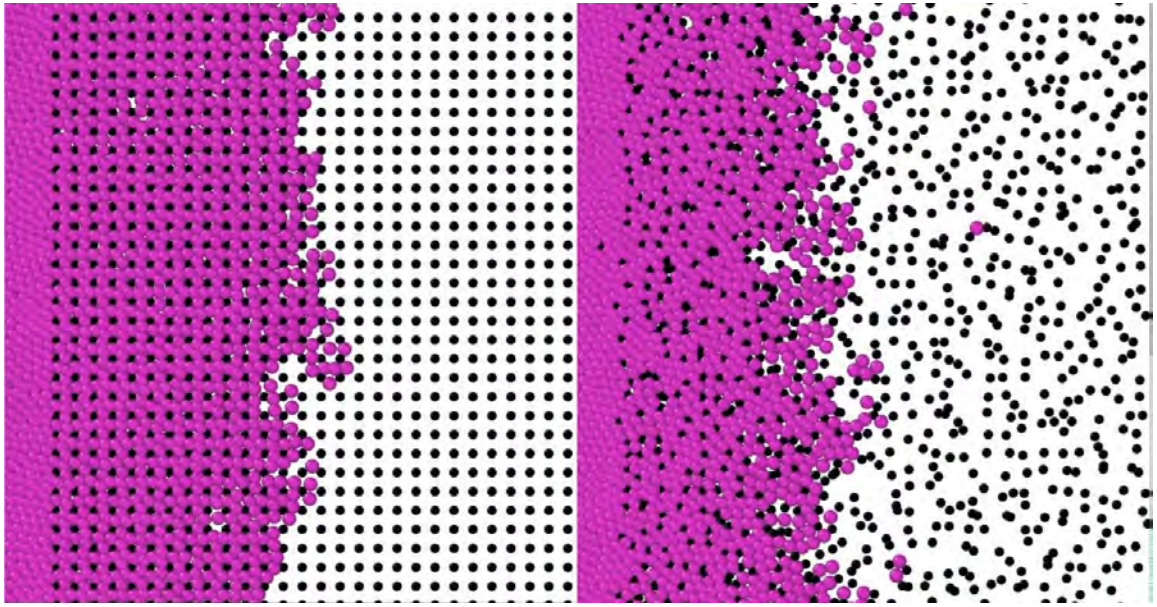

How does this work? Which features of heterogeneity facilitate detachments?

Environment heterogeneity increases rate of detachment

Constraining parameters:

- **single cell parameters** - trajectories of detached cells (F_p, D_r, bias)
- **Interaction parameter (ε)**~ velocity ratio of bulk vs. detached cells; confluency without pillars

Simulations:

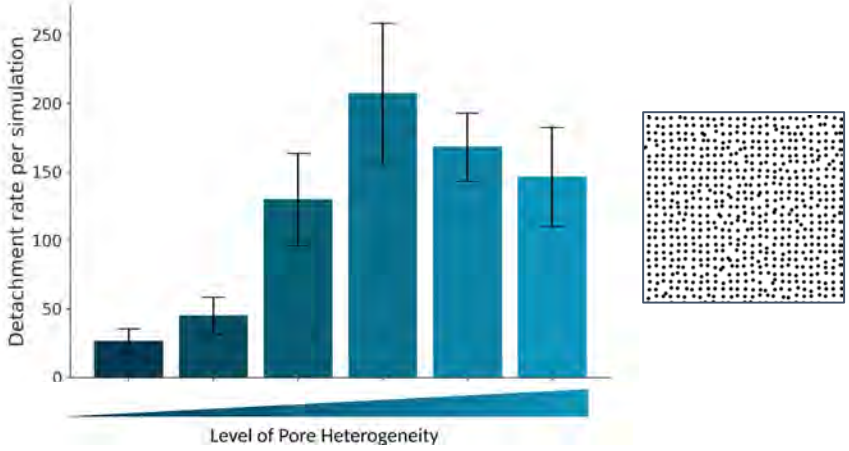

Experiment:

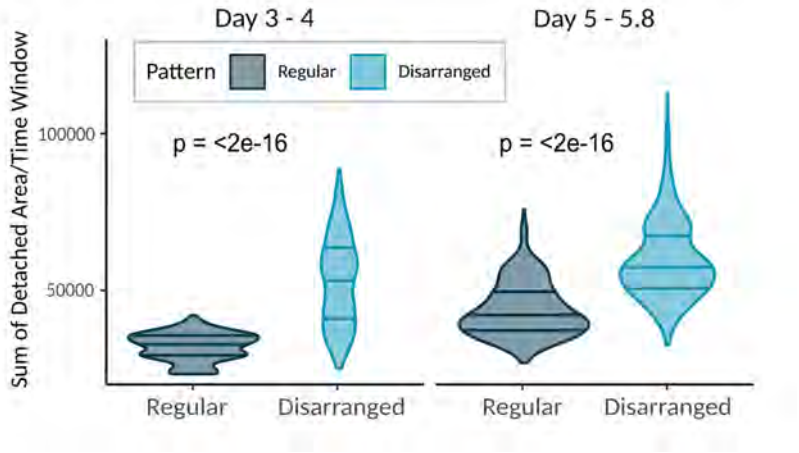

Spatial distribution of detachments

Can we find simple rules without analysing specific pillar arrangements?

→ Detachment events always increase in time!

→ Also consistent “hotspots” across many simulations

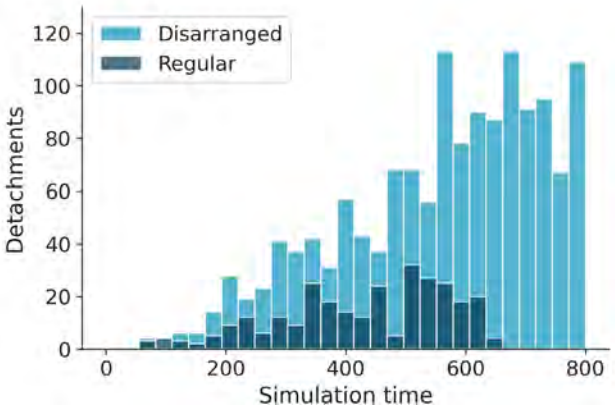

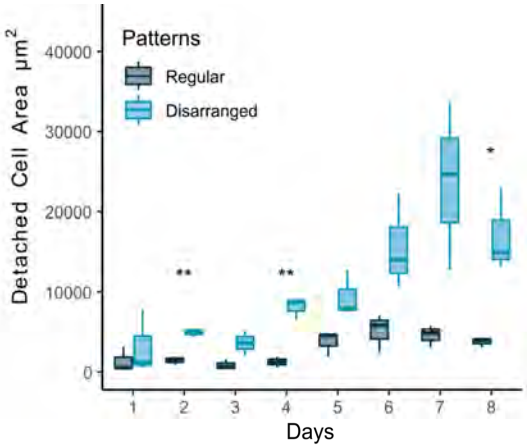

Detachment probability (n=40):

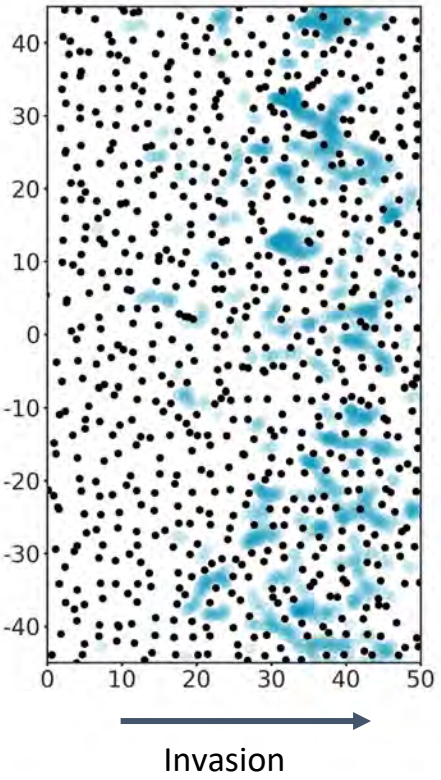

Interfaces **roughens over time** across all conditions…

… but with qualitatively different scaling exponents!

Free space

KPZ dynamics

β = 1/3

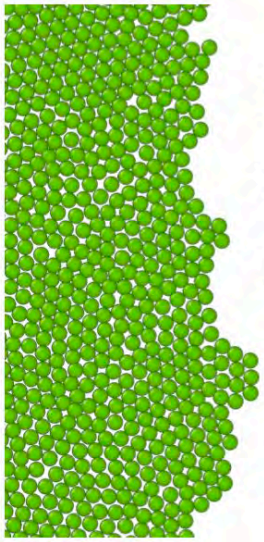

Regular

EW dynamics

β = 1/4

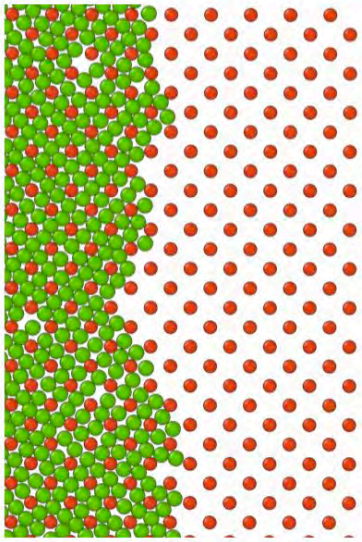

Disarranged

quenched KPZ

β = 0.61

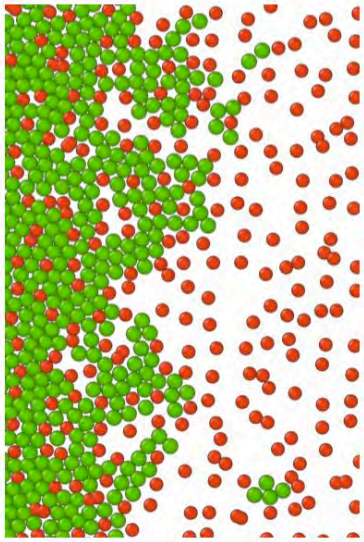

Juraj Majek

EW

$$\frac{\partial h(x,t)}{\partial t} = D\Delta h(x,t) + \sigma\eta(x,t)$$

KPZ [2]

$$\frac{\partial h(x,t)}{\partial t} = D\Delta h(x,t) + |\nabla h(x,t)|^2 + \sigma\eta(x,t)$$

quenched KPZ [3]

$$\frac{\partial h(x,t)}{\partial t} = D\Delta h(x,t) + |\nabla h(x,t)|^2 + \sigma\eta(x,h(x,t))$$

Interfaces **roughens over time** across all conditions…

… but with qualitatively different scaling exponents!

$$W(L,t) = \left\langle \frac{1}{L} \int^{L} \left(h(x,t) - \bar{h}(t)\right)^2 dx \right\rangle^{1/2},$$

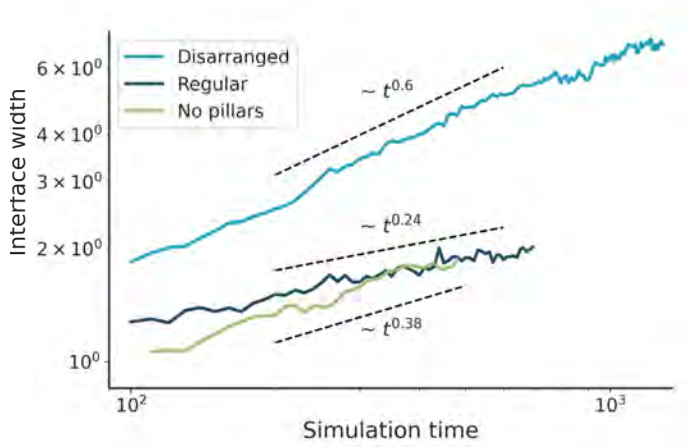

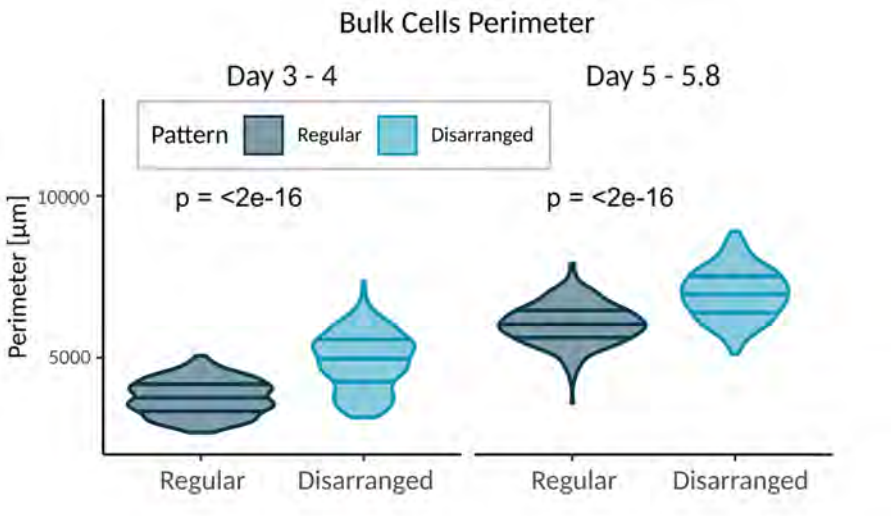

N.Ganai et al, *New. J. Phys*. 21 (2019)
A. Bru et al. *Biophys. J.*, 85 (5), 2948 (2003)

Hypothesis: detachments require a critical interfacial curvature/occurs at the tip regions of the interface

Cells detach at the tips of protrusions

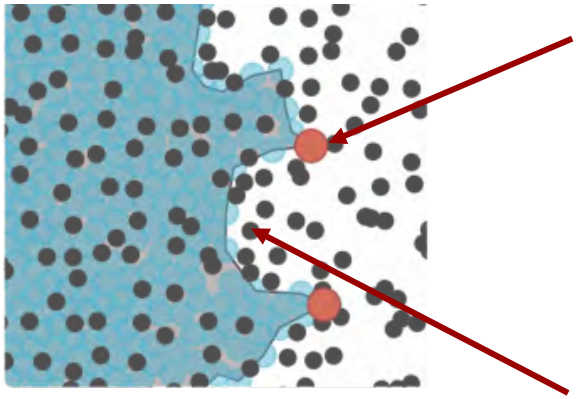

Protrusions (local maxima = 1)

local minima = 0

Relative position of detachments at interface

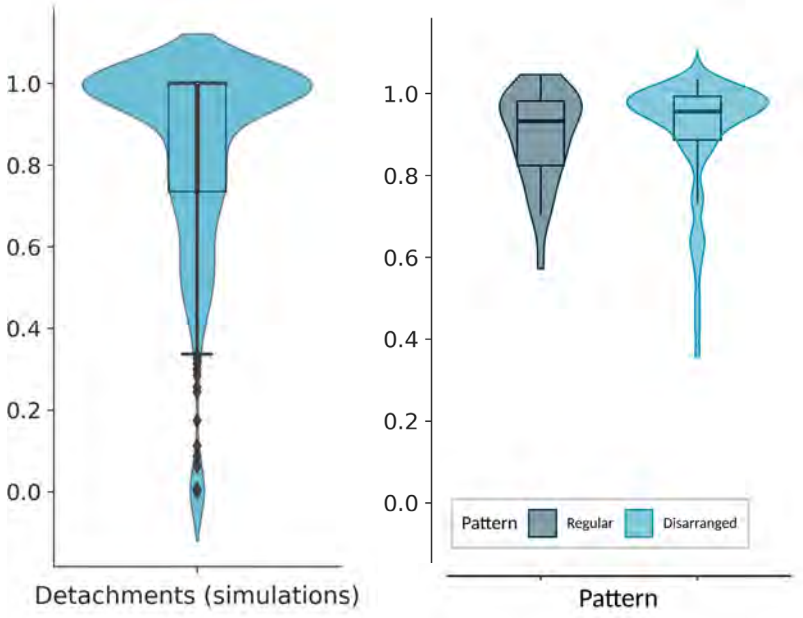

Hypothesis: detachments require a critical interfacial curvature/occurs at the tip regions of the interface

What determines detachments in lateral direction?

Heterogeneity drives protrusions in specific areas

Lateral heterogeneity- geometries creating rough interface

Detachment probability (n=40):

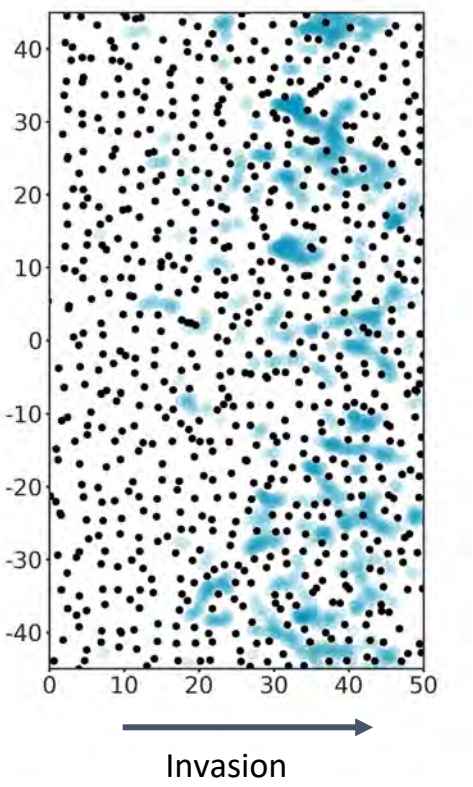

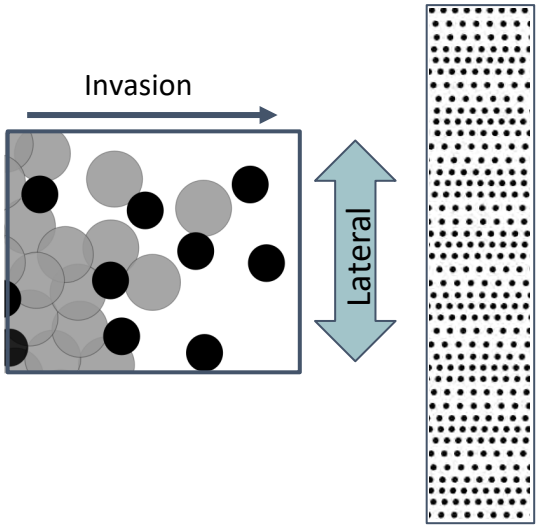

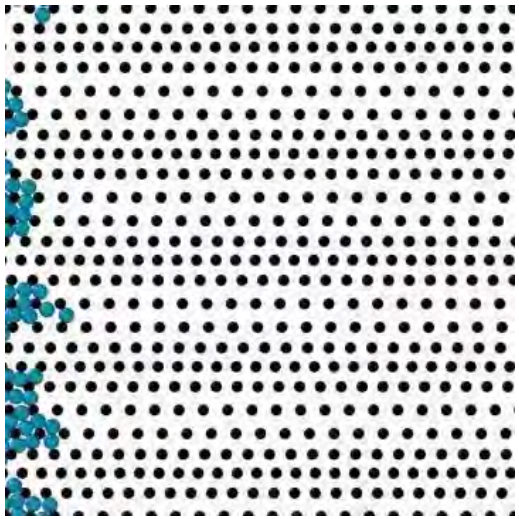

Conclusion 4: Inducing collective to single migration modes via environmental heterogeneity

Detachments induced by disordered geometry

- **Interface roughening** and lateral heterogeneity can explain the global and local detachment pattern

- Complex cellular behavior explored by **simple mechanical model of identical cells** interacting with a **complex environment**

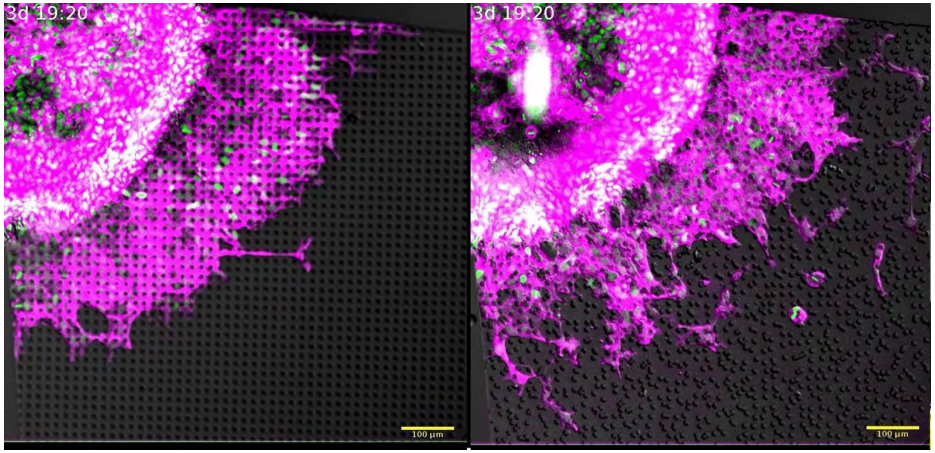

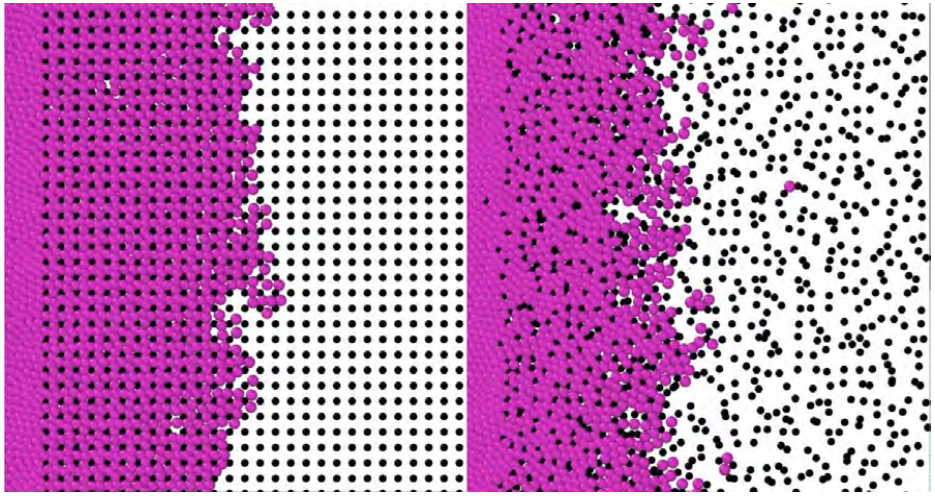

Acknowledgments

2018

2021

2020

2022

Lab members:
Daniel Boocock
Kasumi Kishi
Suyash Naik
Zuzana Dunajova
Mehmet Ucar
Sreyam Sengupta
Preeti Sahu
Andreas Ehrmann
David Bruckner
Uday Ram
Irene Li
Fabrizio Olmeda
Juraj Majek
Paul Robin

Collaborators :
Z. Alsperga, Michael Sixt (ISTA)
E. Vercruysse, S. Gabriele (U Mons)
N. Hino & T. Hirashima (Kyoto)
S. Tasciyan & M. Sixt (ISTA)

IST AUSTRIA
Institute of Science and Technology

European Research Council
Established by the European Commission

FWF
Der Wissenschaftsfonds.

EMBO Young Investigators